STUK

STUK-YTO-TR 189 / NOVEMBER 2002

FEASIBILITY OF GAMMA EMISSION TOMOGRAPHY FOR PARTIAL DEFECT VERIFICATION OF SPENT LWR FUEL ASSEMBLIES

Summary report on simulation and experimental studies including design options and cost-benefit analysis

Task JNT A1201 of the Support Programmes of Finland (FINSP), Hungary (HUNSP) and Sweden (SWESP) to the IAEA Safeguards

Lévai F[1], Desi S[1], Czifrus S[1], Feher S[1], Tarvainen M[2], Honkamaa T[2], Saarinen J[3], Larsson M[4], Rialhe A[5], Arlt R[5]

1 Institute of Nuclear Techniques,
Budapest University of Technology and Economics

2 STUK

3 VTT Processes

4 The Swedish Nuclear Power Inspectorate (SKI)

5 International Atomic Energy Agency (IAEA)

In STUK this study was supervised by Matti Tarvainen

STUK • **SÄTEILYTURVAKESKUS**
STRÅLSÄKERHETSCENTRALEN
RADIATION AND NUCLEAR SAFETY AUTHORITY

Osoite/Address • Laippatie 4, 00880 Helsinki
Postiosoite / Postal address • PL / P.O.Box 14, FIN-00881 Helsinki, FINLAND
Puh./Tel. (09) 759 881, +358 9 759 881 • Fax (09) 759 88 500, +358 9 759 88 500 • www.stuk.fi

ISBN 951-712-613-1 (print)
ISBN 951-712-614-X (pdf)
ISSN 0785-9325

Dark Oy, Vantaa/Finland 2002

LÉVAI Ferenc, DESI Sandor, CZIFRUS Szabolcs, FEHER Sandor (Institute of Nuclear Techniques), TARVAINEN Matti, HONKAMAA Tapani (STUK), SAARINEN Johanna (VTT Processes), LARSSON Mats (SKI) RIALHE Alain, ARLT Rolf (IAEA). Feasibility of gamma emission tomography for partial defect verification of spent LWR fuel assemblies. Summary report on simulation and experimental studies including design options and cost-benefit analysis. Task JNT A1201 of the Support Programmes of Finland (FINSP), Hungary (HUNSP) and Sweden (SWESP) to the IAEA Safeguards. STUK-YTO-TR 189. Helsinki 2002. 50 pp + Annex 10 pp.

Keywords: safeguards, spent fuel, NDA, partial defect testing, tomography

Abstract

Based on the specified need of the IAEA, feasibility of gamma emission tomography has been studied for its potential for non-destructive partial defect verification of spent light water reactor (LWR) fuel by the IAEA. Partial defect verification is required e.g. in cases when nuclear material becomes difficult–to–access. For spent fuel this could mean e.g. the transfer of fuel assemblies into a dry storage. The present requirement for a partial defect method, revealing missing or replacement of 50% or more of the nuclear material, is based on the safeguards criteria. No such methods are, however, available for the IAEA to use for inspection purposes. The results gained in this work by computer simulation and by experimental studies confirm that the gamma emission tomography has potential for a real partial defect verification method for the IAEA safeguards use. An extra advantage, if compared to the present methods used, is that the tomographic method requires no a priori information of the operator declared data. To compare two different design options of a tomography device, also a cost–benefit analysis has been performed. The results gained offer a sound basis for developing a prototype verifier for the inspection use.

Contents

Executive summary

Goals of the study

Spent fuel verification remains one of the most difficult and challenging measurement tasks of safeguards due to high radiation levels and storage locations, which are often under water. The increased long term spent fuel storing, considered difficult–to–access, requires wider and more accurate implementation of verification measures.

A partial defect measurement is needed to verify irradiated fuel assemblies going into difficult–to–access storages. The current detection requirement for such a method is limited to missing of 50% of material. The IAEA does not currently have any measurement system for routine partial defect tests of spent fuel in storage ponds. A tomographic method is proposed for detection of missing or replaced fuel rods in irradiated fuel assemblies at a level well below 50%. A prototype is needed to show feasibility of the method in real inspection use in partial defect verification. The measurement time for such a method should be reasonable and handling should be easy and practical.

This report includes the results of the joint task studying the feasibility of gamma emission tomography for partial defect verification of spent LWR fuel. According to the task outline, it is meant to support the IAEA decision-making on the continuation of the task, i.e. whether to construct a prototype of a tomographic spent fuel verifier or to continue the task in some other ways.

Tomographic (section) imaging method

The basic idea of the proposed methods is mapping of the emitted radiation by imaging techniques. The imaging process consists of two parts: 1) measurement (scanning) of the object, which results in a measured projection data set, and 2) calculation (reconstruction) of a cross section image giving rise to the detected projections. Emitted radiation along different directions is detected by a directionally collimated detector system. The image shows a rod–to–rod distribution of the gamma emitter concentration. Replacement or missing of rods can be revealed by visual or computer based evaluation of the image. In this work, a special scanning system with an analytical special-purpose reconstruction code has been developed to perform the tomographic reconstructions

Simulation studies

Two model types are used to describe the whole imaging process. The straight-line approach assumes a straight-line gamma photon path resulting in a scatter-free projection data set. Scattering is modeled using Monte-Carlo calculations. The calculated projection will be the sum of the two. Gamma-ray source energies used in modeling were 1274 keV (^{154}Eu) and 2185 keV (^{114}Pr). For the calculations, the entire geometry, and properties of detector system was modeled in full detail and are described later in this report.

In order to demonstrate the potential power of the method, a typical large size 17×17–25 PWR assembly (25 water filled rods/positions in an array of 17×17 fuel rods) is simulated, projection data are calculated and the image is reconstructed. Evaluation of the image provides information about the detection capability of missing or replaced rods as well as possibilities and limitations for making measurements in water and in the air.

The basic idea of the technique applied in this work is that a cross-section activity image of an assembly is calculated from the projection data. Calculated activity in the positions of missing or replaced rods has a value lower than the activity of normal rods but, in case of the inner rods, is never equal to zero. This decrease of the activity level should be detected.

To determine whether this decrease is due to a missing rod or not is based on an evaluation procedure. Several factors, including statistical noise, were taken into consideration. A threshold level can be determined from the activity histograms. Rod activities above this level will be considered as relating to normal rods while those below this level will be considered as related to missing rods or rods replaced by dummies, respectively.

Based on the histograms of rod activities, two possibilities can be considered:

- The activity density functions of normal and missing rods can be separated in which case a visual evaluation is possible.
- There is some overlapping between the two activity density functions, in which case only a compromise solution exists for selection of the threshold.

In the latter case the probability of detecting a missing rod and the probability of a false detection (normal rods are detected as missing rods) should be considered. The separation of the two density functions depends on their width. The width is affected mainly by the statistical noise in the measured projections.

Results of simulation studies

A water channel in the central position of the 17×17 assembly causes a decrease of signal in the measured projection. Depending on the measurement angle, an average value of the decrease is 0.5%, i.e. well below the noise level of the detection system used. By using all the measured 120 angles for image calculation, this will cause an overall decrease of 40% in the final image. This can be above the image noise level, if statistical accuracy of the measurement data is sufficient.

Let us define *detection probability of missing or replaced rods in the assembly investigated* as ratio of the detected missing or replaced rods to the total number of missing or replaced rods in the assembly. Simulation results for a 17×17–25 PWR assembly can be summarized as follows:

- In case of a 1% statistical accuracy of the measured projection data, the image activity of a missing rod can be separated from normal rods in all positions of the assembly. Detection probability almost of 100% can thus be obtained.
- In case of a 3% statistical accuracy, in about 4 inner missing rod positions (of the 25) the image activity level is overlapping with normal rods. Missing of rods from these positions would not be detected. Detection probability is 21/25 = 84%.
- In case of a 5% noise level, in about 19 positions (of the 25) the image activity level is overlapping with normal rods. Detection probability is 6/25 = 24%. Increasing of the threshold, however, would increase the probability up to 52% (13 water rods detected) but it would, in addition, result in a false detection of 1 rod.

The high sensitivity of the method to detect removal of irradiated rods can be explained by the following facts:

- There is no need for a reference data set because the activity map itself provides inherent rod–to–rod comparison of fission product gamma activities.
- The effect of a single missing rod is very small to the scanning data at one orientation, usually lower than the noise level. The image reconstruction process uses all the scanning data for calculating each image point. Noise, the statistical fluctuations in different scanning data, is uncorrelated and the averaging effect improves the signal to noise ratio.

Simulated data was useful in designing the measuring equipment as well as planning and optimizing the measurement parameters.

Measurements with spent BWR/PWR assemblies

A total of 6 BWR assemblies and 2 PWR assemblies have been measured in Olkiluoto in Finland and in Ringhals Sweden. The cooling times of the assemblies varied from 0.5 years to 14 years. Both spent fuel stores, are of wet AFR design, and the measurements were performed under water. The tomographic measurement head was fixed on an operator-owned device, called gamma wagon. Gamma wagon has a fuel assembly position, in which the assembly could be rotated relative to the measurement head to measure projections. Number of projections for BWR assemblies were 48 and for PWR assemblies 120.

Table E-I. *Detection probability (%) of missing inner rod in spent LWR fuel using gamma emission tomography.*

	Detection probability (%) when measured in water, analyzed using direct algorithm			Detection probability (%) when measured in air or water, analyzed using model based algorithm
	Measurement noise			Measurement noise
Assembly design	1%	3%	5%	1%
17×17–25 PWR	~100	84	24–52 *	~100
15×15–13 PWR	~100	96	~80	~100

* At the upper value one rod was falsely detected as missing.

During the measurements, three types of room temperature semiconductor detectors have been used including:

- Cylindrical Si(Li) detectors.
- An array of 10 CdTe detectors, each 10 mm × 10 mm × 1 mm in size with a 20 channel electronics unit (made in the laboratory for research).
- An array of 4 CZT (CdZnTe) detectors, each 10 mm × 10 mm × 1 mm in size with an integrated electronics system (factory product).

Results of measurements

A sensitivity to detect any single rods was achieved in water with all 8×8 BWR assemblies. Normally present water rod was resolved in every assembly. Images reconstructed from noisy projections at a high detector discrimination level resulting in a low count rate and statistical noise about 5% gave also acceptable results.

In cases of 17×17 PWR assemblies, results can be summarized as follows:

- For a short-cooled assembly (0.5 a), the high energy ^{144}Pr gamma radiation was measured. Despite pulse pile-up in the detection system caused by the very high gamma radiation level, all single fuel rods could be detected. All the 25 water channels could also be detected in addition to the eight burnable absorber rods. Detection probability of missing rods was 100%.
- For a long-cooled assembly (7.5 a), about 9 of the 25 water channels did not provide a detectable decrease of the signal. Detection probability of missing rods was 16/25 = 64%. The statistical noise in the measured projections was estimated to be 3–4%.
- The measurement geometry used was not optimal: a thick water layer and a limited scanning length caused problems during the evaluation. Due to the short scanning length, the background subtraction was inaccurate resulting in some additional errors and a model-based evaluation was not possible. Only direct image calculation could be performed. The measurement arrangement can be improved significantly, when a more optimized prototype is used.
- Despite the poor measurement geometry the total number of undetected rods (9) represents only about 3% of all the fuel rods of the assembly measured. In addition, the low burn-up rods and stainless-steel replacement rods could clearly be detected.

Comparison of simulated and measured projection data

Scatter-free projection data can be calculated using the straight-line simulation software. Scattering profile and data can be calculated either by Monte-Carlo calculations or by extracting from the measured data, if the measurement geometry is exactly known. For all of the measured assemblies, it has been possible to fit simulated data to the measured data.

Limit of detection sensitivity

The sensitivity limit of a partial defect testing is summarized in Table E-I. The detection threshold is set to a low value to limit the number of falsely detected missing rods to the minimum (around 0). Main conclusions are as follows:

- For assemblies between 8×8 BWR and 15×15 PWR in size, 100% detection probability of missing or replaced rod can be achieved if statistical noise in the measured projection does not exceed 1%. Higher noise level will decrease the probability gradually, but the amount of noise should not exceed 5%. In case of 1% noise, visual evaluation is possible.
- Reconstructed image of large size PWR assem-

blies are very sensitive to noise in the measured projections. Increased statistical noise would decrease the detection probability because missing and normal rod activities would be overlapping.
- Evaluation of an image measured in air (air channel) can be made only with a model-based calculation. With such an algorithm the maximum allowed noise level is 1%.
- In case of measurements with 1% statistical accuracy, the detection probability can be very high both for measurements made in water and in air.

Detection probability of different rod diversion scenarios

The main objective of a partial defect testing is to reveal missing or replacement of rods in an assembly. The probability of detection depends on the number and the positions of rods removed. Main considerations are summarized as follows:

a) Rods missing from outer positions

Any single rod removed from the first two outer rows would be detected with 100% probability. For a 17×17 PWR assembly, there are some 120 rods in these positions.

b) Group of missing inner rods

Removing more rods from neighboring inner positions would be detected with much higher probability than missing of a single rod. Missing of 9 neighboring rods from central positions of a 17×17 assembly would be detected with almost a 100% probability. Also a smaller number of neighboring rods, 4 or 3 would be detected with a high probability.

c) Several single rods missing from inner positions

Removing of rods in positions separated from each other by normal rods can be detected with the same probability as detection of a single missing rod. Therefore, detection of several missing single rods is the most difficult task for the partial defect testing. In the case of a 17×17 PWR assembly, there are some 169 inner positions. By avoiding removal of neighboring rods, some 25 single rods can be removed to make the partial defect testing more difficult.

According to the measurements with 17×17–25 PWR long cooled spent fuel assembly, 64% of the inner water rods (every 2 out of 3) were detected using data measured in a very unfavorable configuration causing about 3–4% of noise. It means that 16 of the 25 water rods were detected, 9 inner water rods were not detected. This is about 3% of the total number of rods in the assembly. The calculations show, that reducing noise level of the measurement, the detection probability would be improved significantly. This can be done using optimum measurement geometry.

Design options for a potential inspection use LWR tomographic verifier

Option 1. *Transportable underwater fork*

In this option the assembly is hanging from the mast of the fuel handling machine in a fixed position during the measurement. The detector-collimator system is rotated inside the watertight, fork-shaped detector head. The estimated measurement time is about 2 × 10 minutes using an array of about 100 detectors. Figure E1 shows a possible schematic design of such a tomographic verifier.

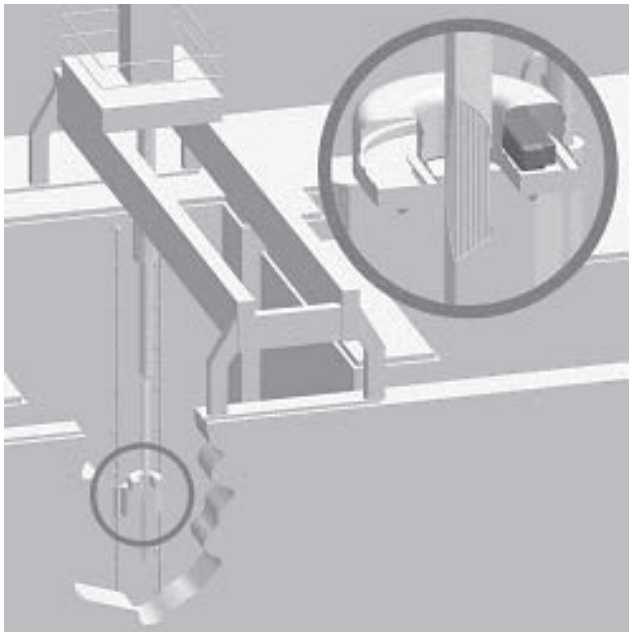

Figure E1. *Fork-design of an underwater tomographic spent fuel verifier. Verifier is attached to the pool wall. The fuel assembly is rotated once during the measurement. Any vertical position of the assembly is verifiable.*

Option 2. *Transportable underwater ring*
In this option the assembly is in a fixed position during the measurement inside the ring-shaped detector head. The moving detector-collimator system is rotated around the whole assembly inside the detector head. The detector head can be placed in a location where the assembly can be moved inside the ring. The measurement time is about 5–15 minutes using two detector arrays, each about 100 detectors. Figure E2 shows a possible design of a ring-shaped tomographic verifier.

Summary of cost-benefit analysis
Based on a cost–benefit analysis, an estimated price of the fork design would be about 220 000 USD and about 300 000 USD for the ring device, respectively. If the licensing costs of the prototype and the training costs would be included, the total cost would be about 280 000 USD for the fork and 360 000 USD for the ring.

The cost of the detection unit is the dominating factor in the total costs of the both options. All costs have been divided over three years in the analysis.

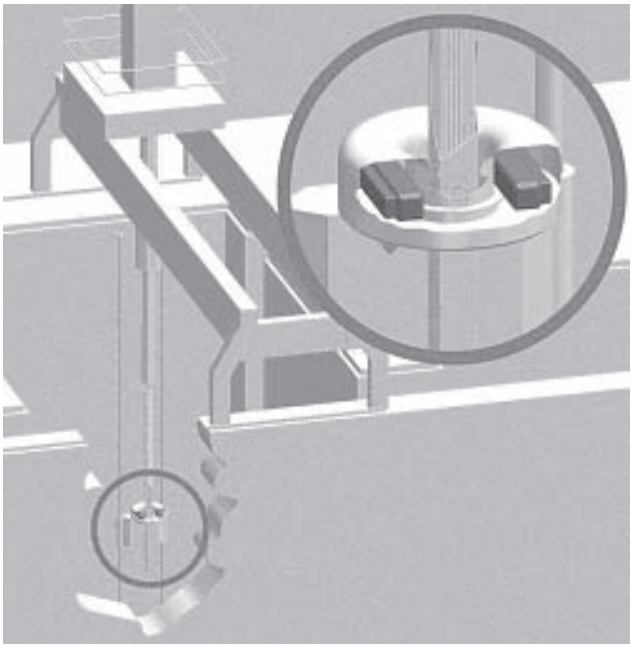

Figure E2. *Ring-design of an underwater tomographic spent fuel verifier. Verifier is attached to the pool wall. The assembly to be measured is moved inside the detector and kept hanging e.g. from the fuel handling machine during measurement. No fuel rotation is needed during measurement. Any vertical position of the assembly is verifiable.*

Verification of 64 assemblies in a campaign would take 5 days using the ring and 7 days using the fork. The use of ring option would be about 4 000 USD cheaper. After about 21 such campaigns the inspection costs would be approximately 84 000 USD less for the ring than for the fork. In other words, after about three years with seven campaigns per year, the ring would become a more economical.

Additional technical options
Adding some extra components into the underwater detector head would provide new features to the tomographic verification system. These components could include:

- A gamma spectrometric system either using some detectors of the array or adding e.g. an extra large-size CZT detector for the gamma spectrometric use.
- Neutron detectors. The detector housing is large enough for positioning two fission chambers in a way similar to the widely used IAEA Fork detector (FDET).

These new elements would give additional data useful both for safeguards and for operational use. They include:

- Axial gamma or neutron, gross or spectral, profiles of the assembly measured
- Excellent averaged gamma or neutron data for the whole assembly due to the fact that measurement are made in very small steps (120 views)
- Azimuthal gamma profiles of the assembly.

Conclusions and proposed next steps of the project
Based on the results of the simulation and experimental studies with several BWR and PWR assemblies, it can be concluded that the tomographic method is feasible for partial defect testing of BWR and PWR assemblies at a single rod level up to assembly size 17×17. This assumes optimum measurement conditions and verifier design and, at the most, 1% statistical noise level in the measurement. Both requirements are realistic.

The method can be used also at a higher statistical noise level (up to 5%) resulting in a detection sensitivity less than one single rod but still about an order of magnitude better that the

present 50% criteria of the IAEA for partial defect test of spent fuel.

Due to the fact that the simulation results have been confirmed by experimental results, it is recommended:

- To design and construct a prototype tomographic verifier.
- To design the prototype based on the ring option.
- To select a test facility, where the prototype and the verification procedures could be used for testing the prototype in realistic conditions.

1 Introduction

In case of light water reactors (LWR), verification of the contents of spent nuclear fuel assemblies is one of the basic safeguards measures routinely carried out by authorities and inspectorates. The basic objective is to gain assurance that the operator declared data concerning isotopic contents and mass are correct. In addition to correctness, also completeness of the data needs to be verified to gain assurance that no material is missing. With introduction of the Integrated Safeguards (IS), increased cooperation between the State systems (SSAC) and inspectorates may offer more flexibility in carrying out the actual measurements. This doesn't, however, change the basic need to create the knowledge first before its continuity can be maintained.

Verification measurements are carried out on different levels depending on the need. Gross defect level measurements result in a conclusion whether the assembly verified is completely missing or replaced with a dummy. If a higher level of assurance of the lack of diversion is needed, partial defect level verification may be needed. The IAEA definition of the meaning of a partial defect has been for years limited by the sensitivity of the methods available to reveal defects. Missing or replacement of 50% or more of the irradiated fuel rods in a spent fuel assembly has been the defined level for a partial defect verification method.

The limited power of the verification methods available for the IAEA to use for spent fuel measurements in field conditions has been known for years. The limiting factor in developing such methods has been technical in nature. No physical or technical principles have been known to allow the development of a practical method for field use by the IAEA. After years of testing and developing different potential methods, as requested by the IAEA, the only passive method available to have real detecting power seems to be the method based on the use of passive gamma emission tomography. When discussing the feasibility tomography, the critical opinions sometimes heard include concerns of the expected high price of such a method, its expected intrusiveness to the operator and its complexity for the inspector to use and draw conclusions. These opinions are understandable but they may be based on a limited evaluation or understanding of all the factors influencing the feasibility of the method discussed. The need for a real partial defect verification method is, however, not ambiguous.

The present task has been carried out in cooperation with the Member State Support Programmes (MSSP) of Finland, Hungary and Sweden. The main responsibility of the technical development has been on the HUNSP. The role of the FINSP has been coordination of the task and support to testing and developing. The main role of the SWESP has been to arrange testing of the method with spent PWR fuel and arranging of alternative analysis of PWR measurement data

2 Goals of the study

Development of the tomographic verification method and evaluation of the feasibility of the proposed principle for safeguards use was started under a FINSP task in cooperation with Hungary already more than ten years ago (1). Results obtained and conclusions drawn were reported accordingly (2–3). Also SWESP has been active in area of tomography of nuclear fuel /5/.

The overall conclusion drawn already before has shown that the tomographic method is feasible for verification measurements of spent LWR fuel. Even missing of individual fuel rods can be revealed under favorable conditions. A detailed evaluation has been requested to allow the IAEA to draw conclusions and to make a decision to construct a device for inspection use.

Development of the detectors and electronics used has been fast during the last few years. The quality of room temperature CdZnTe detectors has enabled improved radiation detection not only in safeguards but also in medicine and other applied fields of science. For safeguards this means improved technical possibilities to design and fabricate detector systems that would be fast to install in facility conditions and sensitive and reliable in practical use.

As a result of the IS concept, the need to verify spent LWR fuel during routine interim inspections of the IAEA may be relieved. In cases categorized as difficult–to–access, the fuel verification needs have, however, remained high. The final disposal of spent fuel brings in a new category of nuclear facilities. In final disposal, one has to prepare for an irreversible disposal process while the facilities may be operational for a period of several decades before closing. To create trust of the absence of diversion, someone has to know the real situation of disposed fuel, preferably on a very high level. A natural high level of knowledge, if possible to reach would be assurance that no individual fuel rods are missing or replaced with dummies.

An additional feature of the security related debate since the fall of 2001 has included a topic of dirty bombs. Not only a real nuclear explosion, as considered earlier, may be needed to create instability and panic. Sub-national terrorist groups using only a small amount of nuclear or radioactive material may reach the same effect. This scenario may significantly lower the required detection level of a diversion from the traditional one significant quantity (SQ) of nuclear material.

Paragraph 3.1 of the Task Outline, "What is needed, why and when", reads as follows: *"A method for partial defect measurement is currently needed to verify irradiated fuel assemblies going to difficult–to–access storage. Current methods available are only able to detect if 50% of spent LWR assembly pins are missing. A tomographic method is claimed to be able to detect if 2% of the pins are missing. It is needed to have a feasibility study, and after that to produce a prototype for practical use, able to do partial defect verification. The measurement time should be reasonable and handling should be easy, practical and method cost beneficial"*.

A further quotation "Consequences if task is not performed", paragraph 3.3 reads: "*The Agency has currently no method of verifying irradiated fuel assemblies for partial defect with high sensitivity. The tomography is a potential method to satisfy this need. The consequence of not having such a method would result in fuel going into difficult–to–access storage without accurate verification.*"

The report below is written in the form requested by the Agency. Based on the results achieved both using simulation and experimental studies, the Agency will receive all technical data needed to make a decision whether to proceed to

the next step to build a prototype device.

The basic idea of the proposed methods is mapping of the emitted radiation by imaging techniques. The common element for all these techniques is detection of the emitted radiation using a directionally sensitive detector–collimator system followed by an image reconstruction (Fig. 1 and Fig. 2). The reconstructed image gives a rod–to–rod distribution of the gamma emitter concentration of the object. Replacement or missing of irradiated fuel rods can be detected by visual or by comprotation upported evaluation of the image.

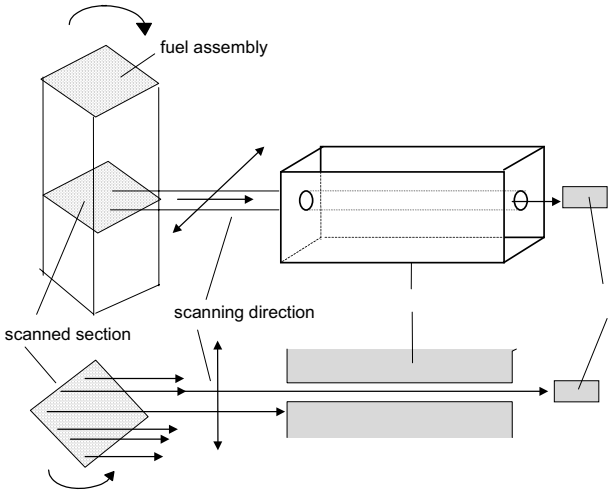

Figure 1. *The principle of diametrical scans of a fuel assembly using a one-detector system.*

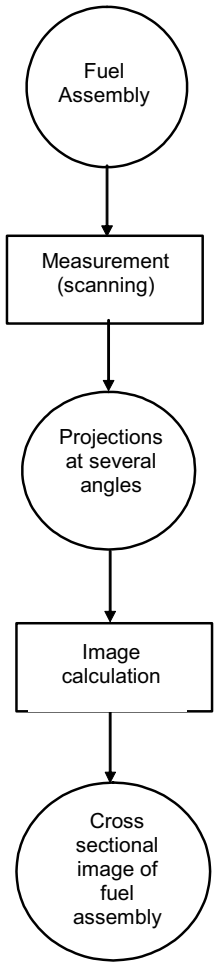

Figure 2. *The tomographic cross-section imaging process.*

4 Summary of simulation and experimental studies

4.1 Description of simulation algorithms and procedures

4.1.1 Simulation model

Simulation is an opposite process to image calculation. The input is a known section image (activity and absorption distribution), the result is the projection data set. To describe the whole imaging process, two model types are used. The straight-line approach assumes a straight line for the gamma photon path and it will result in a scatter-free projection data set. The scattering is modeled using Monte-Carlo calculations. The calculated projection will be the sum of these two (Fig. 3).

4.1.2 Straight-line simulation

The program calculates projections of an arbitrary fuel assembly configuration. The input of the program consists of

- the geometry of the assembly (rod diameter, center–to–center distance, number of rods)
- activity and attenuation map of the assembly including statistical distribution of both parameters
- detector characteristics (distance and response)
- Poisson noise added to the measured value
- position of the centre of mass as compared to the centre of rotation of the assembly.

Basic parameters and the geometry are summarized in Figure 4. A modified version of this program can simulate also hexagonal VVER-type fuel assemblies.

4.1.3 Monte-Carlo calculations

Computer program

Monte Carlo calculations have been performed using the code MCNP4C. This three-dimensional coupled neutron–photon–electron transport code makes it possible to simulate physical phenomena very accurately. The geometry of the system can be described as precisely as required. There are different tally types, such as current, flux and energy deposition estimators. The signal of detectors can be modeled with the aid of the pulse height tally. In order to speed up convergence, a great number of variance reduction techniques are built in the program and can be turned on using input options. The output provides the user with various useful information on the statistical behavior and hence the quality of the tally results.

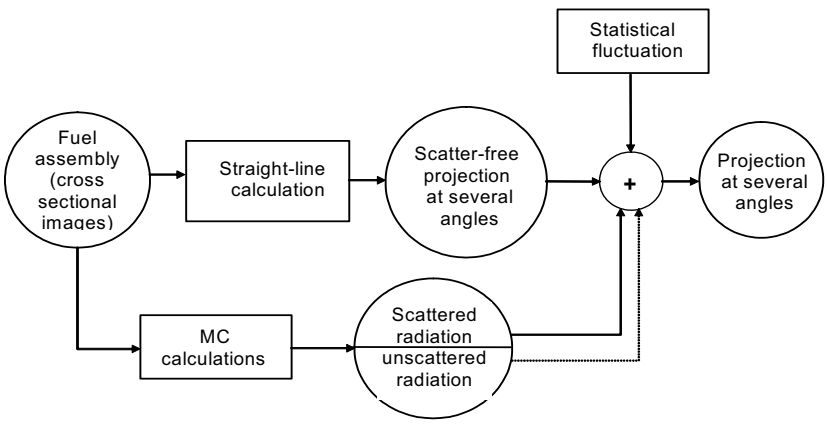

Figure 3. *The simulation model using a straight-line model and Monte-Carlo calculations.*

Computational model

For the MCNP calculations, the entire geometry of interest was modeled in full detail. The model contains the fuel rods of an assembly with cladding, water, lead collimator with slits and CdZnTe detectors. The total width of the collimator is 40 cm, with 100 slits and 100 detector elements placed behind the collimators. The height of the model is 25 cm, which was proven to be sufficient by sensitivity calculations.

The calculations were performed for two distances (see Fig. 5) and three assembly rotations, namely side view, corner view and an intermediate 22.5 degree rotation. The energy distribution of the source photons was chosen so that it simulated the presence of ^{134}Cs, ^{137}Cs and ^{154}Eu. Each detector element was defined as a volumetric photon flux estimator. The photon flux was detected in 9 energy bins between 400 and 1300 keV.

By use of a special option, the photons arriving to the detector elements were flagged according to the number of collisions they had undergone. In this way it was possible to separate the photons

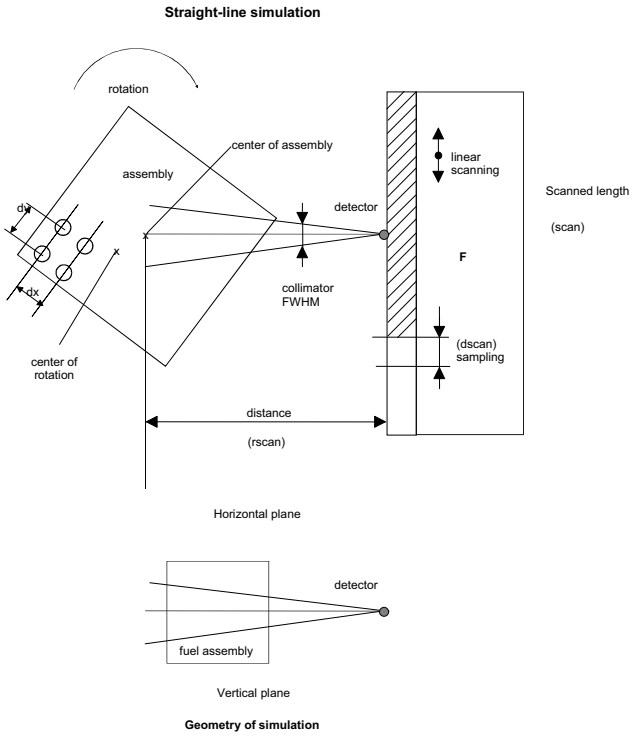

Figure 4. *The basic parameters of the straight-line simulation model used.*

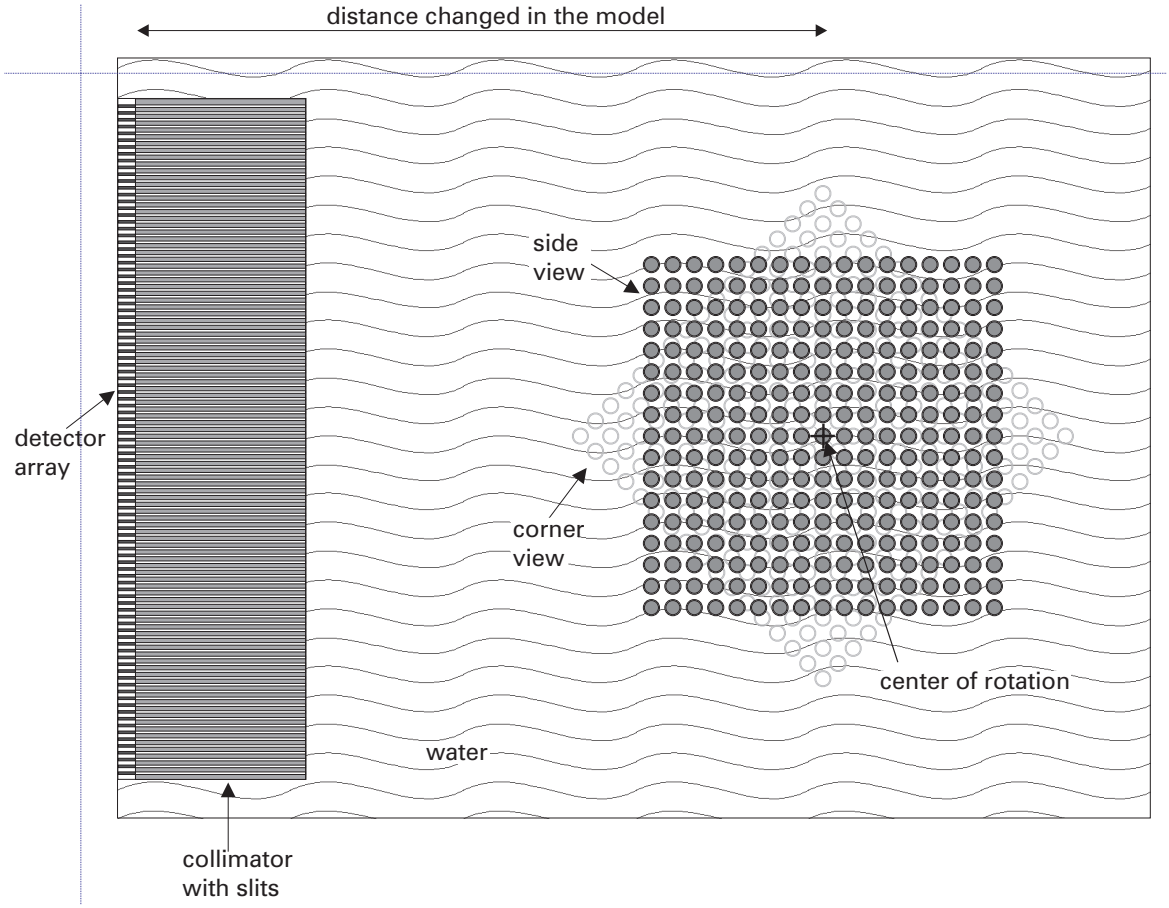

Figure 5. *Geometry of Monte–Carlo calculations (horizontal plane).*

which arrive at the detectors without collisions (unscattered particles) from the ones undergoing one or more collisions. Furthermore, each of the six cases studied (i.e. each rotation and distance combination) was calculated twice: in one calculation the lead was taken as real material, while in the other one the lead of the collimator was taken to be totally black (as if it was of infinite density). After the runs had been completed, the following photon quantities were determined for each detector element:

- total flux of photons
- photons without collisions through the slits
- photons without collisions through the lead collimator
- photons scattered anywhere, passing through the slits
- photons scattered anywhere, passing through the lead.

The conversion of photon fluxes into detector signals was carried out in subsequent calculations using the pulse height tally. By calculating the detector response for sources of photon energy distributions obtained from the above cases, it turned out that the difference between the detector responses for the most different energy spectra was less than 5%. This result was obtained for the discrimination level of 400 keV. Since the statistical uncertainty of the above listed photon flux values were between 4 and 10%, the flux values were taken as directly proportional to the detector signals and were used as such.

4.2 Simulation studies with BWR and PWR assemblies

4.2.1 Signal and background

By definition, the signal is the radiation emitted from the assembly and reaching the detector along a straight-line path. Its energy is above the energy threshold, and its path to the detectors is within the field of view determined by the collimator slit. The slit width is 1.5 mm, the collimator length is 100 mm. All the other gamma rays detected can be considered as unwanted background.

The main components of the background (Fig. 6) are the following:

- direct transmission through the lead collimator (1)
- scattered radiation attenuated by the lead collimator (2)
- scattered radiation reaching the detector within the field of view (3).

The third component of the scattered radiation reaches the detectors without attenuation. The total scattered radiation is the sum of the components 2 and 3. The total background radiation is the sum of components 1, 2, and 3, respectively.

For PWR assemblies measured in water by far, the largest dominating component of the background is the scattering in water. This is due to the fact that the water layer between the assembly and detector may be high. In many cases this limitation cannot be changed.

4.2.2 Simulated cases

In order to determine the potential power of the method to reveal diversion of irradiated fuel rods, several cases have been studied using simulation. The cases studied include the following:

- 8×8 BWR assembly with an inner water channel,
- 17×17 PWR assembly with two inner water channel,
- 17×17 PWR assembly with stainless-steel rod replacement,
- 17×17 PWR assembly with low burnup rod replacement, and
- 17×17 PWR assembly with heterogeneity in the peripheral row
- 17×17 PWR assembly with 25 inner water channels.

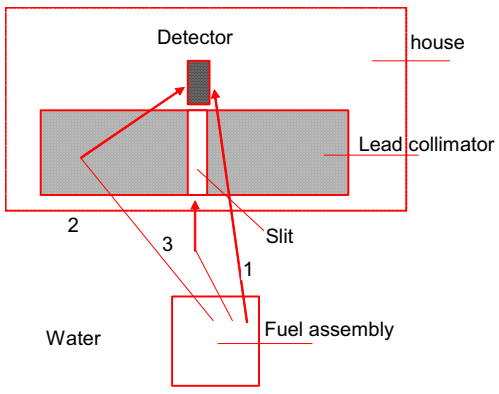

Figure 6. *Main components (1–3) of the background radiation.*

The last case, 17×17–25 PWR, is shown in Figure 7.

Projection data have been calculated and the image reconstructed. Evaluation of the image provides data for the probability of detection and false detection (normal rods are detected as missing rods) as well as for evaluating the possibility to make measurements in the water and in the air. Input data for the geometry have been derived from the measurements. Directional characteristics of the detector have been derived from the detector–collimator used in measurements. Poisson noise has been added to projection data 1%, 3% or 5%.

4.3 Measurement plans based on simulation

4.3.1 Criteria for detecting missing or replaced rods

Image calculation (reconstruction)

Several types of algorithms have been tested to fulfil requirements for imaging spent fuel assemblies. The algorithm developed is a special one with main features:

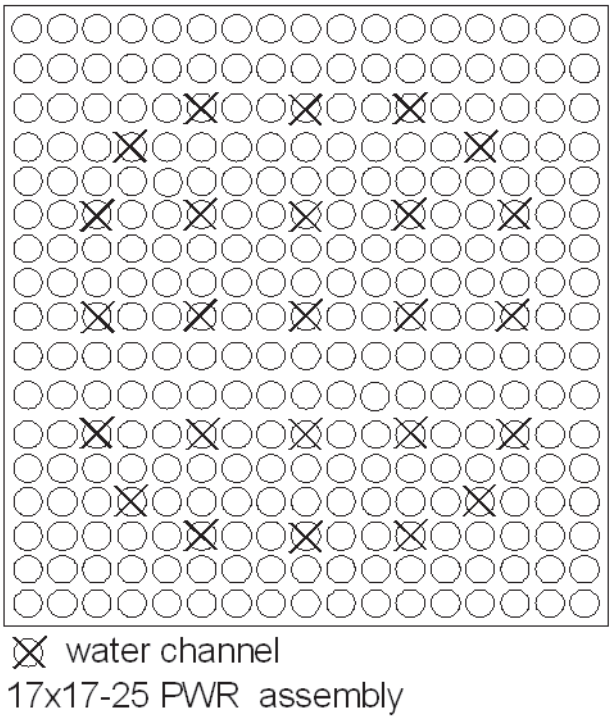

Figure 7. *Simulated case 17×17–25 PWR showing the fuel design and the position of the missing 25 fuel rods (water rods).*

- High resolution analytical image reconstruction with contour detection and with some local tomographic capability.
- Signal to noise improvement capability by filtering and averaging projections over all measured views.
- Effect of scattering can be reduced significantly by separation of signals of different spatial spectra
- Similar improvement can be achieved for reducing the effect of water attenuation profile.

The input for the calculation can be measured projections only (direct image reconstruction) or a priori information can also be used (model-based image reconstruction).

The reconstructed image gives a rod–to–rod distribution of the gamma emitter concentration. Replacement or missing of irradiated fuel rods can be detected by visual or by computer supported evaluation of the image.

Image evaluation

a) Visual evaluation

In cases where the activity decrease is significant, visual evaluation of the image is possible. This is the case for BWR assemblies, short-cooled PWR assemblies and for detection of missing peripheral rods (2–3 outer rows) in any assembly. Visual evaluation is the simplest method for detection.

b) Differential imaging

For those fuel assemblies where all the rods are irradiated in the same fuel cycle, the rod to rod distribution of burnup is a slowly varying function. This means that no large differences are expected between neighboring normal fuel rods. In the image reconstruction calculation, each rod is compared to its neighboring rods and only the difference is imaged. A homogeneous assembly will yield a homogeneous differential image except for peripheral rods which have high activity level due to comparing their activity with the zero-activity level outside. This image evaluation will concentrate on the inner rods, which are the most difficult cases to image. Evaluating the peripheral rods is not a problem because visual evaluation is possible.

The result of a differential image reconstruction will look like all the peripheral rods would have a high activity level.

c) *Fitted envelop function*
A two dimensional function (surface) is fitted on the local peaks of the image function. The local peaks are the rod activity values on the image. These rod activity values will have a distribution around the fitted function described by a density histogram.

Tools for image evaluation (incorporated into the software)

a) *Image histograms*
A histogram is a density function of the image pixel activity. Its integral is the distribution function i.e. the number of pixels having an activity level higher than x. Two histograms can be calculated for the image. One is for all pixels of the image, the other for rod activities only. Distribution functions can be calculated for both. These density histograms will be characterized by a relative standard deviation, which depends on the noise in the measurement (besides algorithm and other factors in the measurement). The higher the noise, the larger the relative standard deviation.

b) *Image activity distribution*
Activity distribution can be displayed along any marked lines on the image. Vertical and horizontal lines can be selected. It is also possible to rotate the image during the image calculation, in cases other than vertical or horizontal lines should be selected.

c) *Threshold image*
A standard window technique can be used for displaying an image between two selected window levels. Activities below the lower level will be set to the low threshold level, those higher the upper threshold level will be set to the high threshold level. The image is displayed between the two levels.

Definitions

- *Threshold level* can be determined from the activity histograms. Modeled rod activities above this level will be considered as relating to normal rods while those below this level will be considered as related to missing rods or rods replaced by dummies, respectively.
- *Detection* of missing or replaced rods means that there are rod positions with an activity level below the threshold level. Rods with an activity level higher than the threshold will be considered as normal rods.
- *False detection* occurs, when normal rod is regarded as a missing or replaced rod. It happens, when imaged activity level of a normal rod falls below the theshold level i.e., when treshold level is set too high.
- *Detection probability of missing or replaced rods in the assembly investigated* is the ratio of the detected missing or replaced rods to the total number of missing or replaced rods.

Criteria for detection

In case a water channel resides in an inner position of the assembly, the reconstructed activity on this position will not be equal zero. This is an artifact of the imaging process used. Evaluation process is needed to determine whether the reconstructed activity decrease is due to a missing rod or not. In the evaluation, several factors, including the statistical noise, should be taken into consideration. For peripheral rods reconstructed activity can be zero and a visual evaluation of the image is possible. Histograms of rod activities are calculated and two possible cases can be considered. These are demonstrated in Figure 8.

In Figure 8 a, the activity density functions of the standard and missing rods are separated. In this case the visual evaluation is possible. In Figure 8 b, the two density functions are somewhat overlapping. A low threshold level can be determined (see later) based on the overlapping part and the image is displayed. Due to overlapping, only a compromise solution exists. Shifting the threshold to the highest value will result in a high detection probability of revealing missing rods i.e. all the missing rods can be detected. This will, however, also result in a high probability of false detection. In case the lower threshold is selected, the probability of revealing missing rods will be decreased i.e. only a certain part of missing rods would be detected but the probability of false detection will be decreased.

Overlapping or separation of the density functions of normal and missing rods of an image depends on the width of the density function (see Fig 8). Important factors influencing this width are as the following:

- Inaccuracy of the algorithm (this is a systematic error),
- Noise level of the measured projection (high noise level will result in a wide density function),
- Features of the algorithm, especially its noise suppression parameters Several algorithms have been compared concerning parameters (width) of the density function. This property is one of the most important parameters in selecting the algorithm.

4.3.2 Calculated scanning parameters

The inaccuracy of the image reconstruction technique used depends strongly on the size of measured data set i.e. the number of projections and sampling points per projection. An important parameter is the resolution requirement to see each rod in the image. To satisfy this requirement, a certain amount of data is needed. The number of projections and sampling interval in the projection are related parameters. Based on the evaluation process, these parameters were calculated. It is assumed that the best available algorithms are available and a single rod detection level is the objective. The calculated parameters to be used for the measurements are as follows:

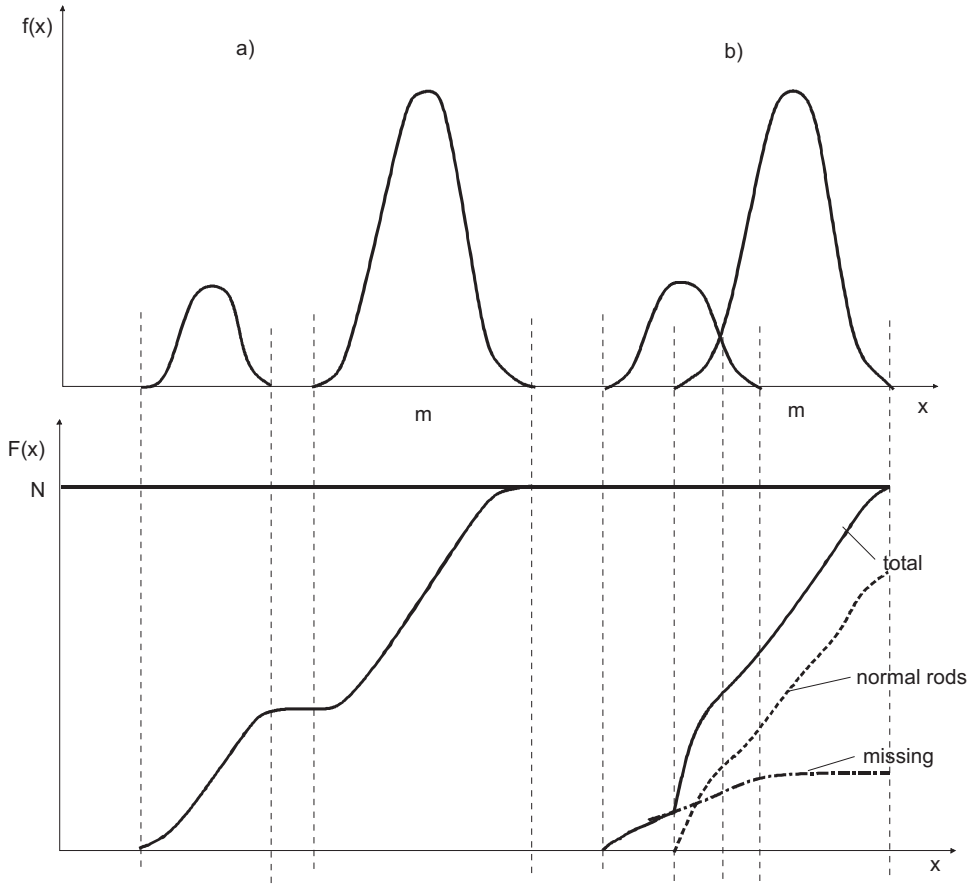

Figure 8. *Histograms showing a modeled normal rod activity and a decreased activity caused by missing (or replaced) fuel rods. Figure a) shows histograms separated and Figure b) histograms overlapping, respectively. f(x) = activity histogram,* $F(x) = \int_0^x f(x)dx$ *is distribution function, x = rod activity, N = total number of rods in the assembly.*

Table I. *Declared parameters of the measured spent fuel assemblies.*

No.	Assembly ID	Measurement date	BU (MWd/kgU)	CT (years)	Fuel channel	Type	Site
1	9016	November 1990	33,2	3,5	no	BWR 8×8–1	Olkiluoto
2	8368	June 1991	31,6	2,1	yes	BWR 8×8–1	Olkiluoto
3	6130	June 1991	24,9	8,1	yes	BWR 8×8–1	Olkiluoto
4	7055	January 1993	17,7	9,5	yes	BWR 8×8–1	Olkiluoto
5	13285	December 1999	30,89	6,5	yes	BWR 8×8–1	Olkiluoto
6		December 1999		14	yes	BWR 8×8–1	Olkiluoto
7	51K	March 2001	39,1	7,5	no	PWR 17×17–25	Ringhals
8	15S	March 2001	42,2	0,5	no	PWR 17×17–25	Ringhals

- BWR 8×8 assembly: 48 projections and 2mm sampling interval,
- PWR 17×17 assembly: 120 projections and 2mm sampling interval.

Larger the number of views and finer the sampling, the higher the needed accuracy of the measurements (geometry, movement etc.) and longer the total time required for scanning. This fact limits practically the number of projections and sampling interval.

4.4 Measurements with spent BWR and PWR assemblies

4.4.1 Characteristics of measured fuel assemblies

A total of 6 BWR assemblies and 2 PWR assemblies have been measured including both short and long cooled assemblies. Declared parameters of the measured assemblies are summarized in Table I. Item no. 7 has 8 burnable absorber rods at the periphery. Item no. 8 is a 0.5 years cooled high burnup (42.2 MWd/kgU) PWR assembly with 25 water filled rods inside. In addition, it includes 3 low burnup rods replaced on one outer row as well as two stainless steel rods replaced on the same outer row.

4.4.2 Experimental set-up and measurements

Hardware arrangement and data

The spent fuel storages used for measurements, both in Olkiluoto Finland and in Ringhals Sweden, are wet AFR storages for BWR and PWR fuel assemblies. Both are equipped with an operator owned fuel lift equipment, called gamma wagon that is used for fuel service purposes. The gamma wagon is attached on a fixed position to the wall of the fuel handling pond. Different fuel service fixtures can be clamped to the gamma wagon allowing the operator to move the assembly in vertical direction and also to rotate it manually. The measurement fixture used for tomographic studies holds the assembly during measurement. Figure 9 shows the overall measurement arrangement used.

The tomographic detector head, with the backside opened in Figure 10 was attached to a fixed position in the middle of the measurement fixture before lifting the equipment into the pond. Figure 11 shows the measurement geometry of the assembly inside the fixture as it was during the measurements. The fuel handling machine was used to transfer the assembly into the fixture.

Detectors

Three types of room temperature semiconductor detector have been used. First, two cylindrical Si(Li) detectors of different sizes placed in a row, one behind the other, measuring the same point of the assembly. In Figure 12 the size of the second detector is in brackets. The pulse processing electronics has been developed and produced in the research laboratory of the Budapest University of Technology and Economics, BUTE (formerly Technical University of Budapest, TEB). Second, an array of 10 CdTe detectors, each 10 mm × 10 mm, in size has been used with the same electronics to shorten the measurement time. Third, an array of 4 CZT detectors has been used for measuring the PWR assemblies. The operation principle of the electronics used for the CZT detectors is the same, but it is operating in a factory produced integrat-

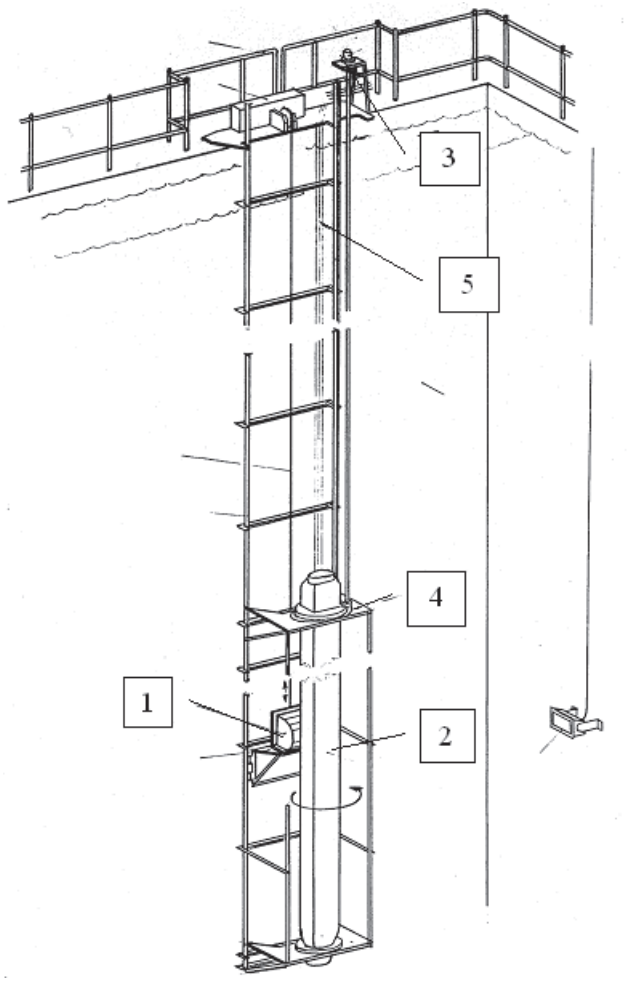

Figure 9. *Schematic measurement arrangement used during tomographic measurements at the AFR storages in Finland and in Sweden showing measurement head (1), fuel assembly (2), fuel rotation equipment (3), measurement fixture attached to the gamma wagon (4) and cables (5).*

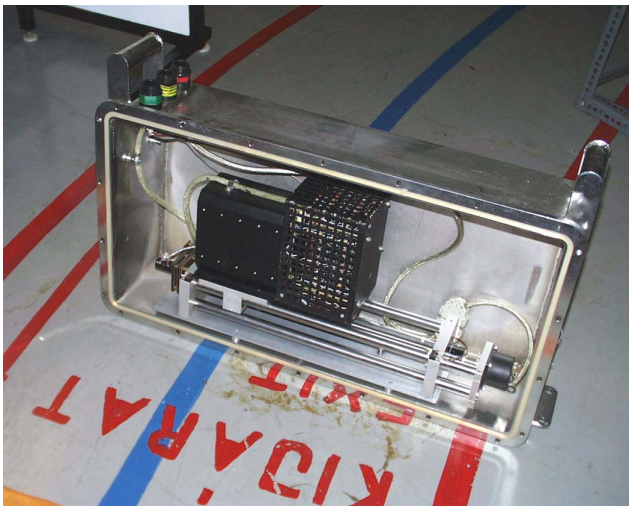

Figure 10. *An opened underwater detector head used for tomographic measurements of spent fuel assemblies.*

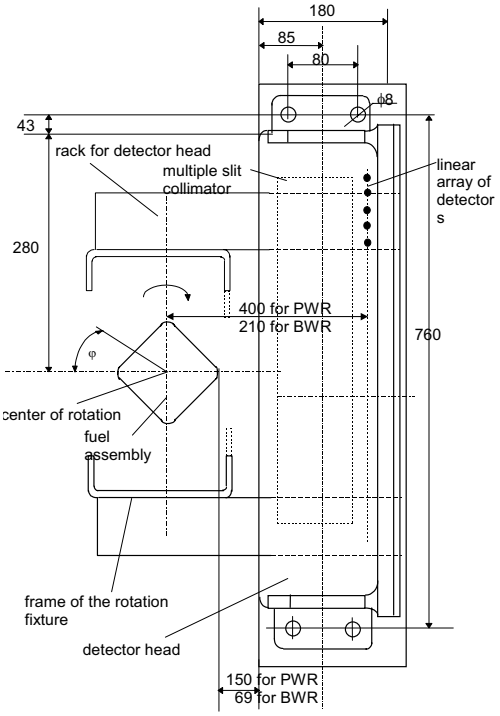

Figure 11. *Measurement geometry (top view) of the tomographic measurements of BWR and PRW fuel assemblies. The stainless steel made detector head was attached to the measurement fixture.*

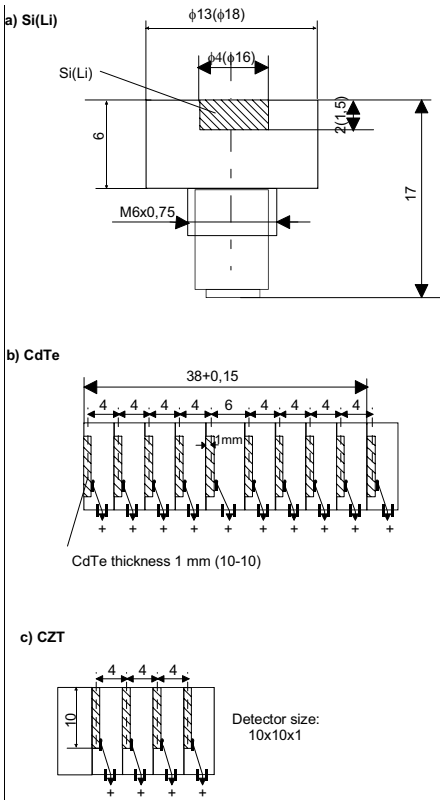

Figure 12. *Room temperature detectors used for tomographic measurement.*

Table II. *Scanning parameters used during tomographic measurement campaigns of spent LWR fuel.*

	Measurement campaign		
Parameter	**BWR 1**	**BWR 2**	**PWR**
Number and type of detectors	1 Si(Li)	10 CdTe (array)	1+3 CZT
Scanning step	2 mm	20 mm	6 mm
Sampling interval	2 mm	2 mm	2 mm
Number of measured views (angles)	32	48	120
Distance from detector to assembly center of rotation	210 mm	210 mm	410 mm
Total scanning time	5 h	1 h	10 h

ed system. Size of detectors used is seen in Figure 12. Table II includes listing of the detectors and their settings for different measurement campaigns.

Single detector scanning for detector calibration

The detection system was moved mechanically in 2 mm steps during measurements. The same approach was used for all campaigns and for all detectors. Each detector measures the same projection and scanning results are stored for each detector separately. These scanning results are used to determine the differences in the detector performance (sensitivity etc.) and calculating the calibration factors to compensate for these differences. This calibration was done once after energy discriminator level calibration.

Multidetector scanning

The detector array is moved mechanically in predefined steps. Movement of the array is programmed to cover the whole measurement area with the measurement interval of 2 mm. A computer program calculates the composed scanning file for the 2 mm sampling. Calibration to compensate for differences in the detector sensitivity is needed to obtain an artefact-free scanning profile. Calibration factors are measured using a single detector scanning for this purpose.

Discriminator level setting

The size of the detectors is so small, that full energy absorption probability of incoming gamma radiation is negligible. Therefore, counts observed at the compton edge are used as a signal. The energy level threshold discriminators control the pulse amplitudes at the output of the analogue amplifier. Two discriminator levels for each detector channel are set. The lower threshold level discriminator (U_{D1}) is set to measure the ^{154}Eu and ^{144}Pr gamma rays together. The higher threshold level discriminator (U_{D2}) is set to detect only the gamma rays of ^{144}Pr.

The image of the gamma rays above the higher threshold level can be used for short cooled assemblies only (cooling time, CT < 3 a) to provide images of gamma rays of short-lived ^{144}Pr. The image of gamma rays above the lower threshold level can be used for long-cooled assemblies providing information of the distribution of the ^{154}Eu gamma-ray emitter concentration. The discriminator levels are used to select the measured part of gamma-ray spectra. The closer the discrimination level is to the Compton edge of a selected gamma ray, the better is the energy selectivity of the system. This is limited by statistical error.

4.4.3 Summary of scanning data

Details of the scanning data differ somewhat for different measurement campaigns. Table II shows scanning parameters used in different cases. Table III shows the discriminator levels for different detectors and measured fuel assemblies.

4.4.4 Summary of data analysis methods

Model-based calculation and extraction of information

The large background caused by scattering in water and the incorrect background subtraction due to a limited scanning length necessitate adding of more information to the image reconstruction process of PWR assemblies. A physical model of the scanning process is being developed, which provides some additional information for the image reconstruction. In addition, there are several useful parameters, which can be extracted from

Table III. *Discriminator levels (U_D) for different detectors and measured assemblies.*

Detector	Cooling time of measured fuel assemblies (a)	UD (keV)	Fuel design
Si(Li)	2,1	973	BWR
Si(Li)	3,5	700	BWR
Si(Li)	8,1	620	BWR
CdTe	9,5	250	BWR
CZT	6,5	900/1300 *	BWR
CZT	14	900/1000 *	BWR
CZT	0,5	1700/2000 **	PWR
CZT	7,5	400/700	PWR

* High level due to increased noise (grounding problem).
** High level due to pulse pile-up.

the measured data set. Some of the elements of this model are introduced below.

a) *Water attenuation profile*
Due to the large thickness of the water layer between the assembly and the detector, the measured data set is modulated by the water attenuation profile. This attenuation profile and its correction function can be calculated if the geometrical parameters (rod diameter, pitch) of the assembly are known.

b) *Background subtraction from measured data*
After calculation, it can be concluded the scattered radiation profile is a slowly varying function. Separation of it is thus possible which can result in a scatter-free profile. Geometrical parameters (rod diameter, pitch) of the assembly containing all the rods should be known for this calculation.

c) *Fuel absorption correction*
A mathematical model is used to correct for the absorption. Due to the instability problem, only a limited improvement is possible. For imaging purposes it can, however, be significant.

Direct image reconstruction

Direct image reconstruction means that the input is only the measured data set file. No other data are needed. The main advantage of these types of image reconstruction is that the distortion caused by incorrect data can be avoided. The main drawback of these techniques is that normally the measured sinogram data set for such a high absorbent, like the assembly, is never good enough for accurate imaging. As an example, a map of attenuation coefficient (which in tomography is measured by a separate imaging process) is not available for the image calculation made in this report.

Model-based image calculation

The water attenuation correction and the model-based scattered background subtraction can be included in the algorithm. In case of an accurate model, the data image can be improved. Any incorrect a priori data, however, would introduce distortion and error in the imaging process resulting in faulty detection.

5 Results

5.1 Simulated cross section images of BWR and PWR assemblies

5.1.1 Signal and background

Calculated activity profiles for the side view of a BWR and a PWR assembly are shown in Figures 13 and 14. Contribution of the unscattered and the scattered gamma rays to the detected signal is shown. For these demonstrations a detector discrimination level of 400 keV is used.

Calculation results for a side view of a PWR (17×17) assembly show clearly the strong effect of the scattered gamma rays (Fig. 14). Due to a large water layer between the assembly and the detector and a very thin collimator used in the head, the intensity of the scattered radiation is by far larger than the signal. This profile has been calculated for several other views as well and the signal–to–background ratio was found to be similar.

5.1.2 Effect of water rods on measured data

Figure 15 shows a PWR assembly with three water channels located 1) in the center of the assembly, 2) in a middle position and 3) in a corner position. The missing rod (water channel in this case) will result in a decrease of the signal in measurements where its position is within the collimated view of the detector. This decrease will depend on the path-length of the line along the collimated view in the assembly. In case the line along the collimated view is aligned with the rod rows, columns or diagonal, the path-length in the fuel is longer and the signal decrease caused by one missing rod is at the minimum. On the other hand, if the line of view travels mostly between the rod rows or columns, the decrease is higher. Therefore percentual changes in the intensity of the projections depend on the angle of measurement. Changes based on the simulation results

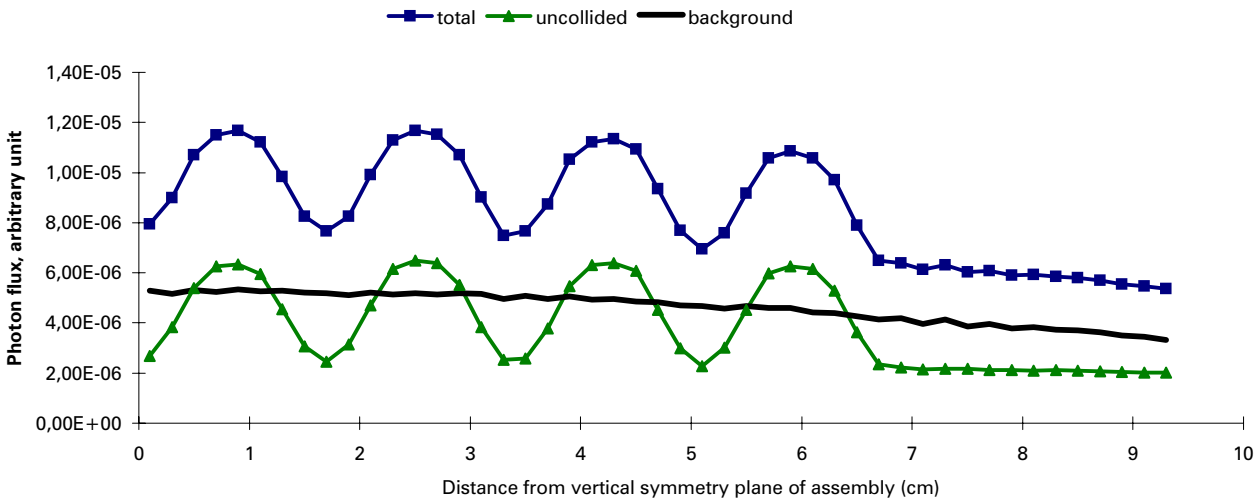

Figure 13. *Side view of a spent BWR assembly showing the contribution of unscattered and scattered photons to the detected signal. Distance between the detector and the rotational centre of the assembly was 21 cm.*

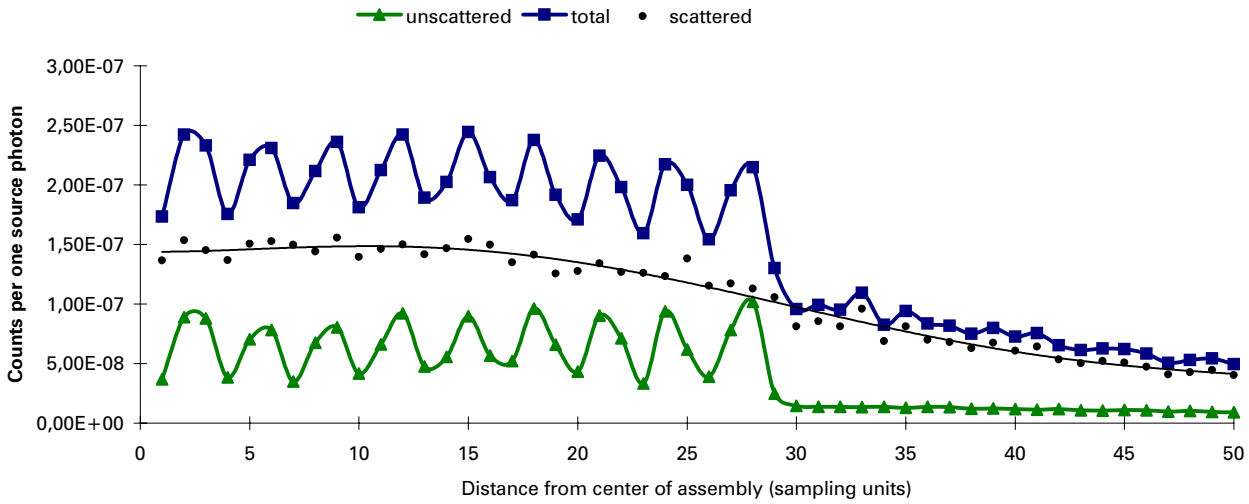

Figure 14. *Side view of a spent PWR (17×17) assembly showing the contribution of unscattered and scattered photons to the signal. Distance between the detector and the rotational centre of the assembly was 41 cm.*

(see Fig. 15) can be summarized as follows:

- center position (1): 0.12…0.9% (average 0.5%)
- middle position (2): 0.12…2.28% (average 1.2%)
- corner position (3): 0.12…97.77% (average 49%).

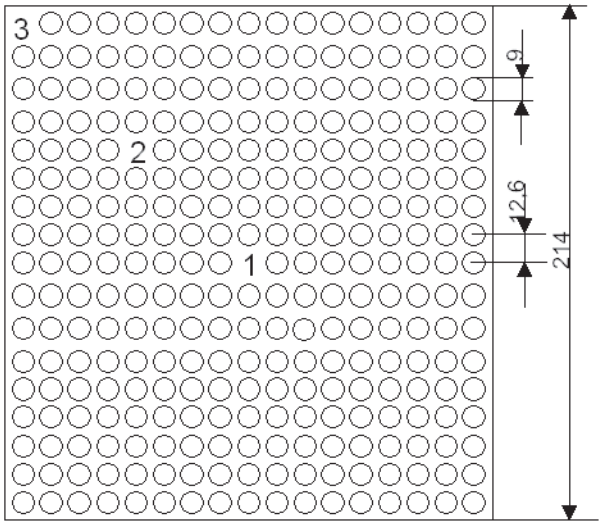

Figure 15. *Simulation studies were carried out using a 17×17 PWR assembly with three water channels in different positions (positions 1–3).*

Except for the water channel in the corner position, all the others are below the level of noise of a good detection system. This is the small signal, which should be extracted from the noise using an image reconstruction algorithm. One of the required features of the algorithm to be used is that it shall sum up all the projections measured at several angles. There is no correlation between the noise of projections measured at different angles but all the small changes in the projections are correlated and will be summed up.

Simulations have been made also for air filled channels and different replacement (dummy) cases. For air channels, the effect is about half of the value of a water channel. For dummies it is several times more than the value calculated for a water channel. Generally speaking, the higher the gamma radiation attenuation of a dummy is, the larger is the effect on the measured projection. A larger effect is also easier to detect.

***Table IV**. The effect of a water rod in different locations (location 1–3, see Fig. 15) of a 17×17 PWR assembly to the activity level in the image.*

Position of water rod	1 (center)	2 (middle)	3 (periphery)
Image activity decrease	40%	60%	90%…98%

5.1.3 Effect of water rods on image

A decrease of the rod activity will be detected in the position of a water channel. This decrease was calculated by a noise-free simulation of a 17×17 PWR assembly with water channels in different positions. The image was reconstructed from 120 views using 2 mm sampling.

Table IV shows that a water channel in the first row (position 3) causes an almost 100% signal decrease (signal level ≈ 0). The effect of the inner positions (1 and 2) is smaller. It is this decrease of the signal that should be extracted from the statistical fluctuations (noise) of the rod activities.

5.1.4 Effect of noise on image

Statistical fluctuations (noise) of normal rod activities of the cross sectional image depend on the statistical fluctuations in the measured projections and on the image evaluation procedures. A 17×17 PWR assembly with only normal rods (no missing or replaced rod) was simulated changing the amount of noise in the measured projections. The relative standard deviation of the image density histograms were calculated using differential image evaluation algorithms. Decrease of the rod activity should be detectable if it is smaller than threshold level determined from the rod activity histogram. Table V shows the results of the simulation.

5.1.5 Evaluation of simulated PWR images

Images reconstructed from the simulations of measurements in water were evaluated by a direct algorithm using a differential evaluation technique. The images can be seen in Figure 16 (a–c). Three histograms were calculated for each image:

- histogram of all rod activities including the missing inner rods
- histogram of normal rod activities
- histogram of reconstructed activity levels in the missing rod positions.

***Table V.** Effect of noise to the relative standard deviation of the rod image density histograms.*

Noise in projections (%)	1	3	5
Relative standard deviation σ/M (%)	14,1	20,6	27,6

The two last activity histograms for the inner rods can be seen in Figure 16 (right) together with the threshold images (left) calculated from the projections with different (Poisson) noise levels. From the simulation it can be concluded that for the case of 1% noise, normal rods and water channels are clearly separated from each other. This is why a 100% of missing rods can be detected even based on visual evaluation.

For the two other cases, some overlapping of activities of normal and missing rods can be observed.

Activities in some positions of the missing rods are on the same level as the activity of normal rod positions. This overlapping is larger for the larger noise levels. In case the threshold is set to the lower value of this overlapping, some of the missing rods will be undetected but there will be no false detections. If the threshold is set to a higher value, more missing rod positions will be detected together with a false detection of some of the normal rods.

To determine the overlapping part of the normal and missing positions, activity histogram distribution functions for the two histograms have been calculated. In the simulated case with 3% noise level, in about 4 missing rod positions the activity level is in the range of the normal rods. In case of 5% noise level, about 19 missing rods would not be detected. In case 1 false detection is allowed, this number will be only 12.

There are several ways to find out the optimum threshold. The best estimate can be obtained from a distribution function. An estimate can be obtained also by subtracting 3–4 standard devia-

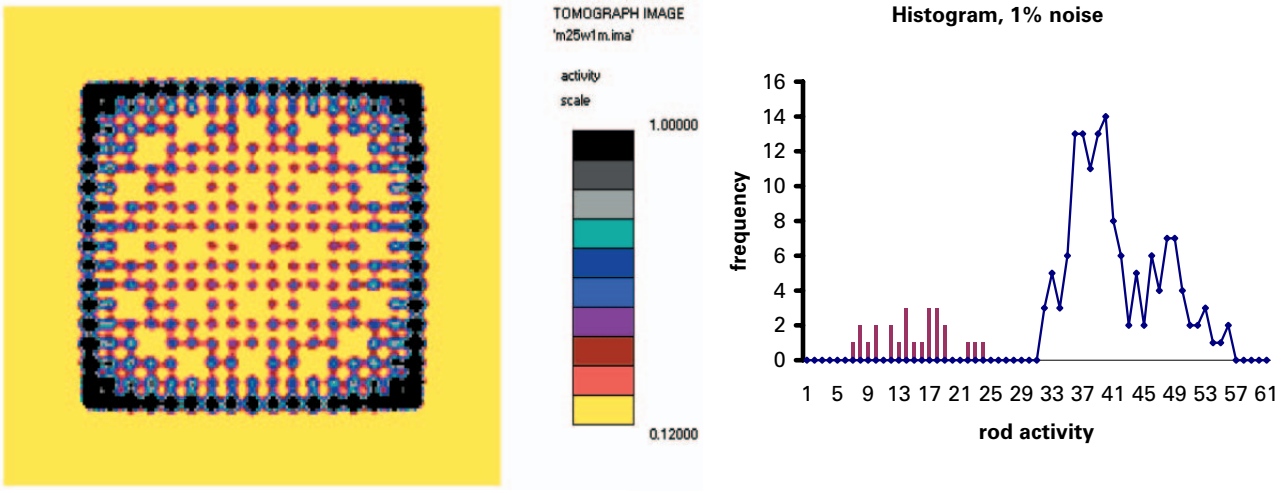

Figure 16. *Reconstructed images for a simulated 17×17–25 PWR assembly (left). Different noise levels have been added to the signal: 1% (a), 3% (b) and5 % (c). Rod activity histograms are shown on the right. Dark bars indicate activities in positions where fuel rods are missing.*

tions from the mean activity level. Both of these parameters can be calculated for the histograms using the software.

5.2 Measured cross section images of BWR and PWR assemblies

Three selected cross section images reconstructed by a direct reconstruction algorithm are shown in Figures 17 (a–c). A differential evaluation algorithm was applied for the PWR image reconstruction. The BWR image can be evaluated even visually.

Figure 17 a) shows a short-cooled PWR assembly. Its cooling time is only 0.5 a (assembly no. 8 in Table I). Activity cross section images of the two longer cooled BWR and PWR assemblies (no.3 and 7 in Table I) are shown in Figures 17 b) and c), respectively.

For all measured BWR assemblies single rod detection sensitivity was achieved. Images reconstructed from noisy projections gave also good results. These noisy measurements were carried out using a high detector discrimination level resulting in a low count rate and statistical noise over 5%.

The results of the PWR assemblies can be summarized as follows:

The short cooling time (0.5 a) of the PWR assembly (assembly no. 8, Table I) made it possible to detect the high energy ^{144}Pr gamma radiation (2186 keV). Due to a low self-absorption and despite the very high gamma radiation level causing pulse pile-up in detection system, a 100% detection result was obtained. All the 25 water channels were revealed together with 8 burnable absorber rods.

In case of the long-cooled (7.5 a) assembly (no. 7, Table I), about 9 of the 25 water channels could not provide a definite signal decrease. Statistical noise in the measured projections was estimated to be 3–4%. The geometry of the measurement was not even close to optimal. A thick water layer and a short scanning length caused problems during evaluation. Due to the short scanning length, the background subtraction was inaccurate resulting in some additional errors. Model-based evaluation was not possible, only a direct image calculation. Despite these limiting facts, which can be significantly improved by measurements with an optimized prototype, the total number of undetected rods (9) means only about 3% of all rods of the assembly measured.

The low burnup rods and stainless-steel replacement rods of the PWR assembly could clearly be detected. These items located even in the first row made the detection of the inner water channels more difficult.

Rod activity histogram of the PWR assembly shown in Figure 17 c) is shown in Figure 18. From verification point of view, this is the most difficult case measured. Detection threshold is calculated from the mean and relative standard deviations (vertical cursor line in Fig. 18). Using a direct image reconstruction algorithm, the calculated activity of about 9 missing rod positions is overlapping with the activity values of normal rods.

5.3 Alternative analysis approach

Uppsala University in Sweden has also performed analysis of the measurement data from the PWR assembly no. 7 (see Table I). An alternative tomographic analysis method was then applied, based on an algebraic algorithm involving detailed modeling of the gamma ray interaction of the emitted radiation from the fuel. This analysis is accounted for in Annex.

It is pointed out in Annex that this method requires exact positioning data of fuel and equipment. Further on, it is desirable to involve spectroscopic analysis of the full-energy peak of the selected decay. Although measurement data were collected without these properties, the analysis offered highly confident detection of the five exchanged rods in the assembly. The ability to detect the water channels, assuming their existence to be unknown was also investigated. Even though the results were considered promising, the precision of the scanning data has to be improved to result in reliable detection. This is in accordance with the results in section 5.2.

5.4 Comparison of simulated and measured projection results

Scatter-free projection data can be calculated by the straight-line simulation software. Scattering profiles and data are calculated by Monte-Carlo calculations but can also be extracted from the measured data if the measurement geometry is known exactly.

a)

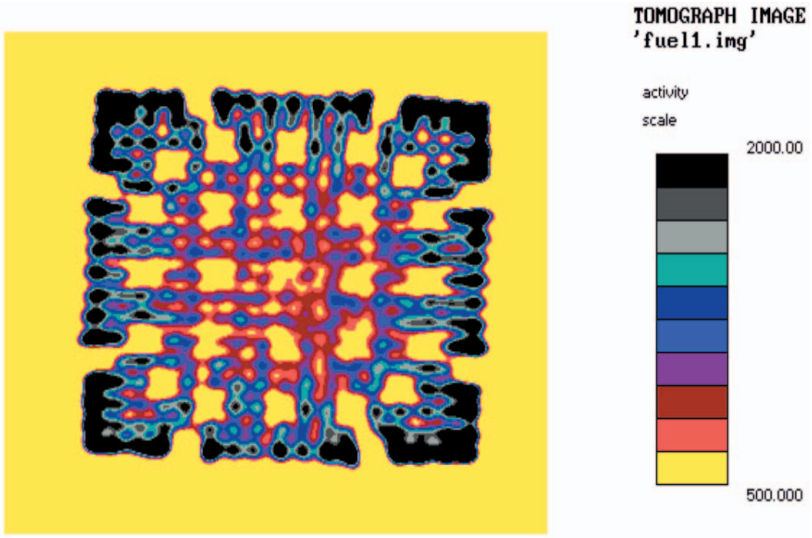

b)

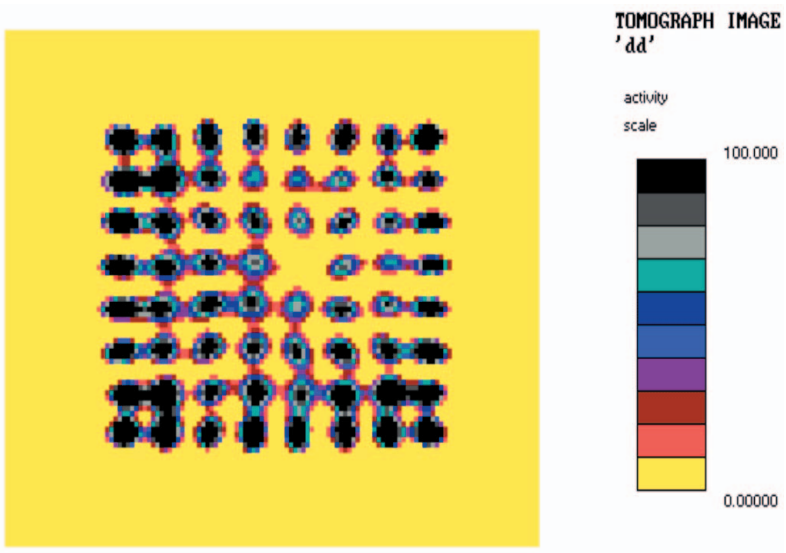

c)

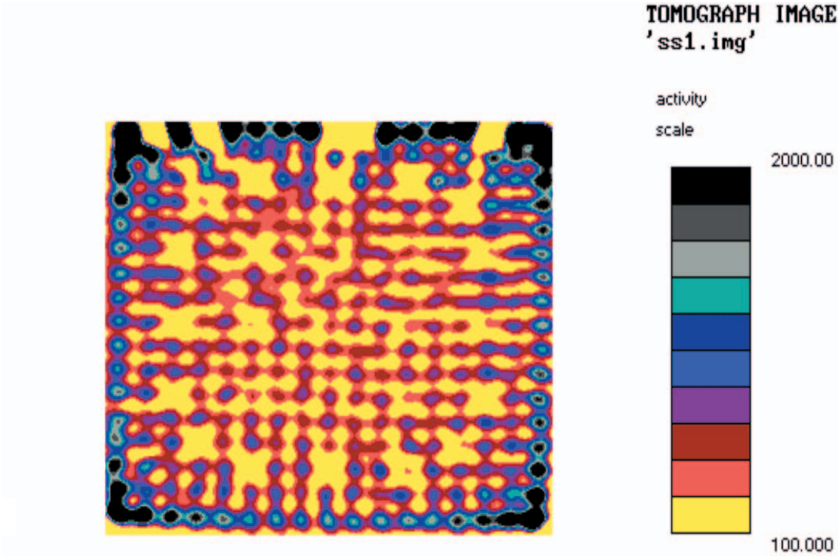

Figure 17. *Cross sectional activity images of measured assemblies: a) a short cooled (0.5 a) PWR assembly, b) a long cooled (8.1 a) BWR assembly and c) a long cooled (7.5 a) PWR assembly.*

Figure 19 shows a simulated scatter-free projection a), a scattering profile b) and a total (sum) simulated projection at a side view of a 17×17 PWR assembly. The projection of 19 c) can be compared with a measured profile shown for the same case in Figure 20. For all of the measured assemblies, the simulated data matches well with the measured data. Simulated data have proved out to be always very useful for planning and optimizing actual fuel measurements.

5.5 Other results

5.5.1 Optimization of measurement geometry

Noise and resolution

For imaging an activity cross section of an assembly with a resolution required to view each rod separately, the required sampling interval can be calculated. This turns out to be about 2–4 mm for PWR assemblies. The sampling interval depends on the collimator slit width and on the distance between the detector and the assembly. When this distance is changed, the sampling interval (and collimator slit width) should be recalculated.

The simulation results related to noise show that the lower the image resolution, the better the signal–to–noise ratio. This is due to filtering out the high frequency (noise) components limiting the resolution.

A recommended practical solution is to use 2 mm sampling interval for the scanning process. Filtering, depending on noise requirement, can be carried out during processing of the measured data. The price to pay for it is that in some cases over-sampling cannot be avoided i.e. longer measurement times and/or more detectors in the array. However, this solution is flexible to changes in the measurement geometry. The same configuration can be used for several geometries.

Scattered radiation background

The scattered radiation component depends on the thickness of the water layer between detector and the fuel assembly. The smaller this distance is the smaller is the background. This has been demonstrated by the results of Monte-Carlo calculations, where the signal and the background have been calculated for two distances between the detector and the assembly center–of–rotation. One of the calculated distances was 41 cm, the distance used during measurements at the Ringhals facility. The second distance is 27 cm which is the smallest possible distance that can be used. There is a big difference between these two cases as can be seen in the Figures 21 and 22.

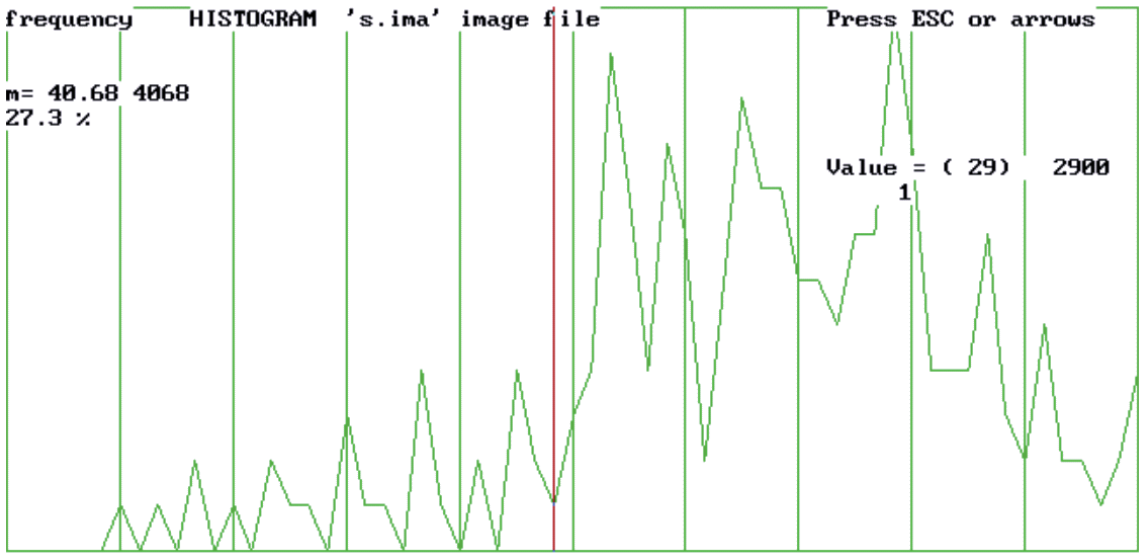

Figure 18. *Rod activity histogram for the PWR assembly shown in Fig. 17 c) including 25 water rods, 3 replaced low burnup rods and 2 replaced steel rods. Calculated activity threshold is shown as a vertical line. All rods are not necessary shown in the histogram, since some may not be visible at all (no local maximum) and normal rods in two outer rows may be excluded.*

a)

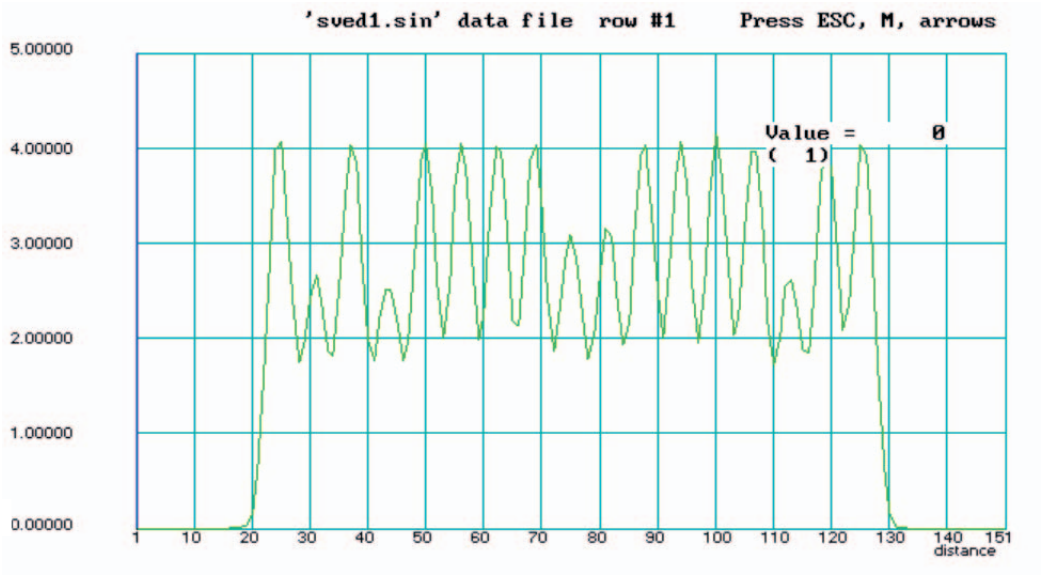

b)

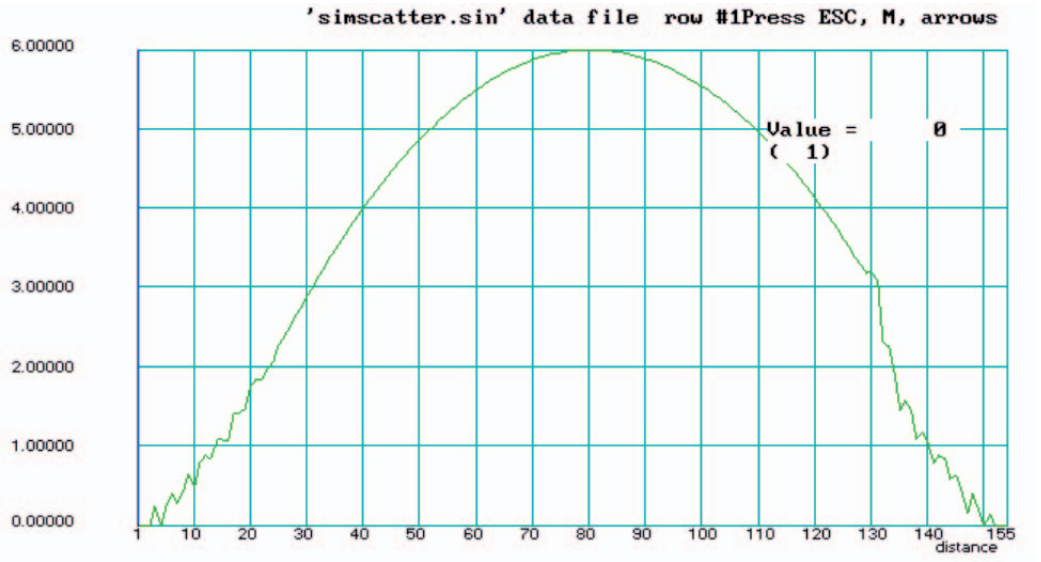

c)

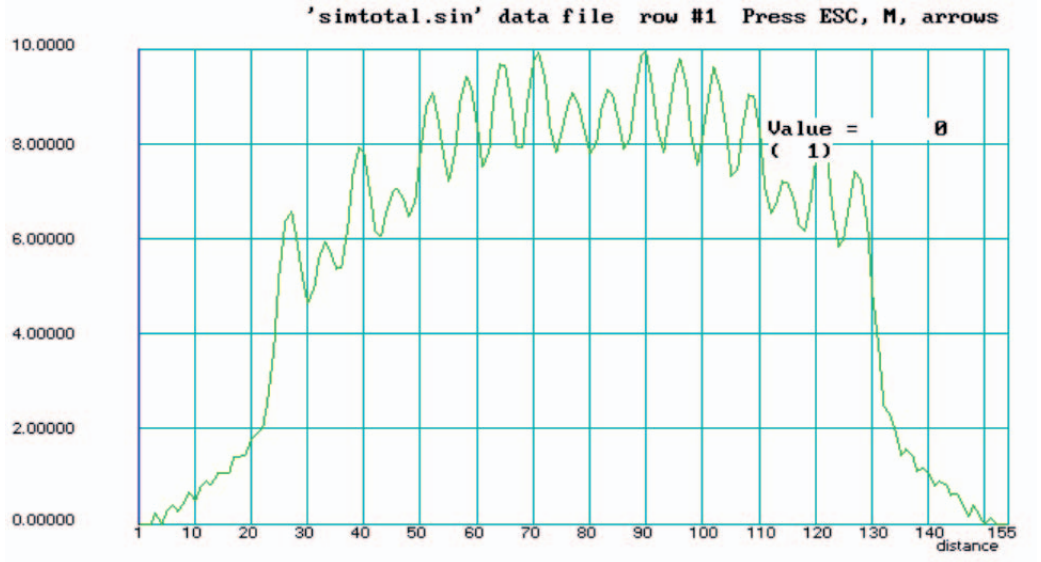

Figure 19. *Simulation side view data for a long cooled PWR assembly: a) a scatter-free projection calculated by a straight-line model, b) scattering profile obtained by model-based calculations and c) the sum of the two, i.e. the total simulated projection.*

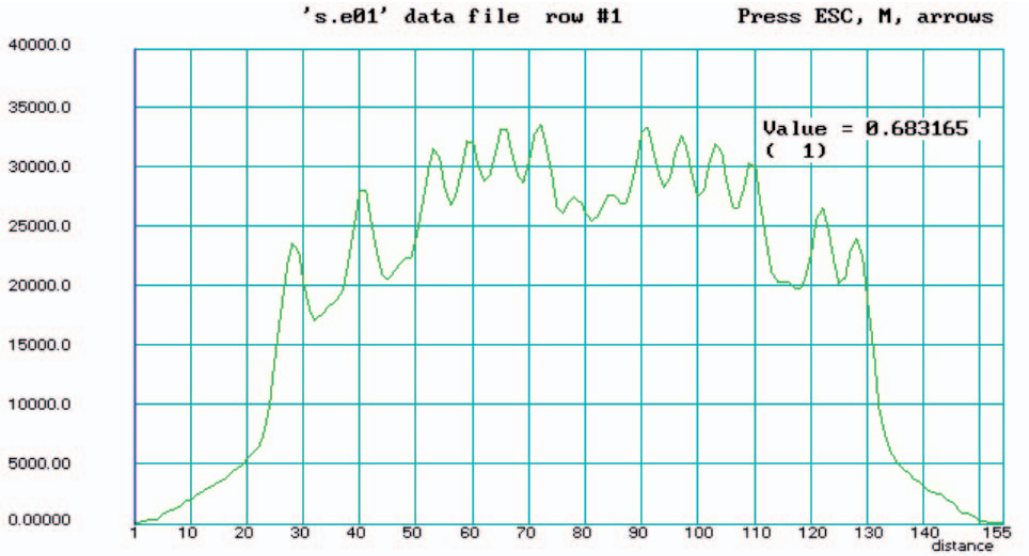

Figure 20. *Measured projections showing a side view of the long cooled PWR assembly (no. 8, Table I). The measured projection and the simulated projection 19 c) present the same case.*

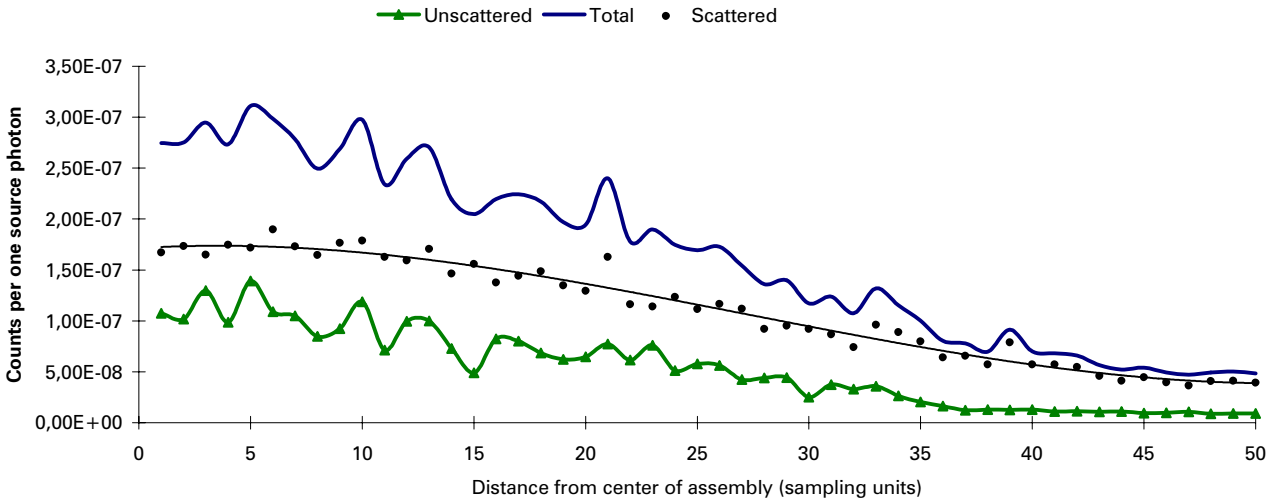

Figure 21. *Contribution of the unscattered and the scattered photon component to the total signal. Corner view of a PWR assembly, water layer thickness 41 cm.*

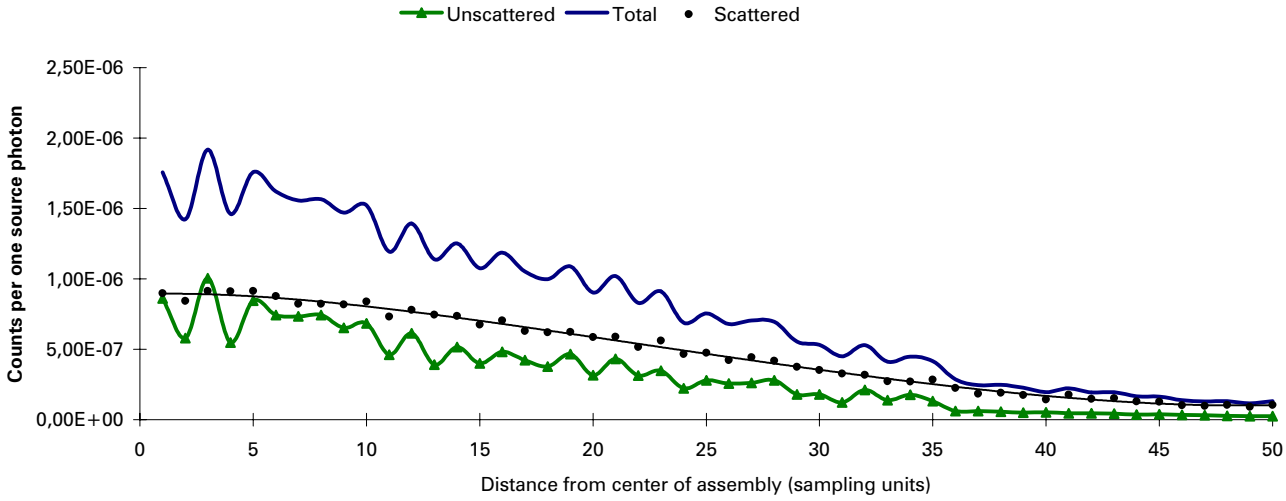

Figure 22. *Contribution of the unscattered and the scattered photon component to the total signal. Corner view of a PWR assembly, water layer thickness 27 cm.*

5.5.2 Influence of scattered radiation to background

The background radiation profile is a slowly varying function. Using a direct image reconstruction algorithm this profile can be separated from the signal with a higher frequency spectrum. This separation is never perfect due to some overlapping of the spectra. The result can, however, be fairly good in practice. In case of a model-based image calculation, the background radiation profile should be calculated and subtracted from the measured projection. The accuracy of the background subtraction depends on the accuracy of the model used. Incorrect data in the model may result in incorrect images.

5.6 Feasibility for partial defect testing (50% missing)

5.6.1 Influence of rod position to detection sensitivity

The activity of each rod position of an image will include some systematic position dependence. This is caused by several factors:

- Attenuation of water will effect the measured projection because the thickness of water along a scanning line crossing the rod depends on the position of the rod in the assembly. This effect is at the minimum if measurements are made in the air. Its influence will be significantly reduced in cases where water attenuation is compensated for, e.g. by using a model-based algorithm.
- Most algorithms used for image reconstruction have some position dependence features. Reconstructed activities of rod positions towards the center of the assembly will be decreasing slightly. This is due to the very high self-absorption of gamma radiation in the fuel material. There are techniques to compensate for this effect. The difficulty lies in the fact that the imaging process is non-linear in nature and any modification in the imaging algorithm may cause unpredictable distortion effects in the image.

Direct algorithms with differential evaluation will result in images with high activity of the peripheral rods and some dependence also on the rod positions other than the first two rows. Sensitivity difference for detection of a water channel in the center positions and in the mid positions of a PWR assembly can be seen in Table IV.

The detection probability for missing rods in the first two peripheral rows is almost 100% even in the case of the largest assemblies. This is why the assembly will be divided in two parts for the image evaluation purposes. They are the outer rods i.e. the rods in two peripheral rows, and the inner rods i.e. all others rods. Evaluation of the inner rods is made separately. There are two ways to realize this separation. One is to cut out the outer two rows; the other is to limit the activity of the image to the value of the inner rods. In the first case a 17×17 PWR assembly is cut into a 13×13 assembly (with only inner rods) for further evaluation. In the second case the activity of outer rods is at the maximum level i.e. black in the color coded image, while the map of inner rods will be unchanged.

5.6.2 Detection sensitivity in water and in air

Factors which have influence on the detection and which are different for measurement in water and in air are summarized as follows:

1. The effect of a water channel on the measured projection is twice as large as the effect of an air channel. This makes the air measurements more difficult. Direct image reconstruction provides much less satisfactory results for measurements in air than for measurements in water.

2. The attenuation of water and the scattered radiation background are missing from the air measurements. This is a big advantage. A simplified model-based algorithm can easily be applied to measurements made in air. At a 1% input noise level it will result in an image quality similar to measurements made in water at a 1% noise level and can be analyzed using a direct algorithm. A model-based algorithm can provide similar, good results for both cases. The maximum 1% limit of the input noise is a requirement for measurements in air.

Table VI. *Influence of the relative rod activity to the image activity at different positions of a PWR fuel assembly (see Fig. 15 for details of position).*

	Relative rod activity	0	0,66	0,9
Decrease of image activity from reconstructed activity of normal rod	Position 1 (center)	100%	75%	25%
	Position 2 (middle)	100%	80%	40%

5.6.3 Detection of low burnup or inactive rods

Low burnup rods

Low burnup fuel rods have a lower gamma activity than normal rods. Examples of these items include:

- Rods irradiated less than normal rods. Gamma activity of the ^{154}Eu in rods is exponentially proportional to the irradiation time. Decrease of 66% in activity will cause an easily detectable decrease of about 75% in the center position of the image (see Table VI).
- Burnable absorber rods. Fuel rods with burnable poisons have an activity level much lower than that of normal rods. Based on the measurement made at the Ringhals facility, an order of magnitude lower activity of a rod containing burnable absorber was detected as compared to normal rods. This, of course, can be easily detected.

If a low burnup rod resides at peripheral position it can be identified and unambiquously distinghuished from a missing rod. However, it may be that tomographic inspection alone is not capable of identifying small number of low burnup rods at center locations. In this special case, some other methods, like weighing, may be needed to achieve rod level accuracy.

Inactive replacement

In this case the item replacing a normal irradiated rod has a zero activity but not zero absorption. From simulation results it can be concluded that the higher the absorption the higher the decrease of the activity level (signal). Detection of fresh fuel rod is the easiest case to reveal. A stainless steel dummy in the center position of a 17×17 fuel assembly will also cause a large signal, which can easily be detected even by visual evaluation of the image.

5.6.4 Absorption and path length

The most important physical parameter, which limits the application of this imaging technique for verification purposes, is the product of the absorption coefficient of the detected gamma radiation in the fuel assembly and the maximum path length of the scanning line in the assembly $(\mu l)_{max}$. It reaches its maximum value when a narrow scanning line is crossing the diameter of all the rods in a row. This is a theoretical parameter due to the fact that the scanning line has a finite width (determined by the collimator) and the maximum path length will be shorter than it is in the case of a narrow line. This parameter is, however, useful in comparing measurement possibilities with different fuel types. The lower this product is the better is the result. It is also true that for assemblies with the same $(\mu l)_{max}$ value, the results are similar.

5.6.5 Measurement time and noise

Based on measurements and simulations it can be concluded that the level of statistical noise in the measured projection plays a very significant role in the detection probability of missing or replaced rods. At the 1% noise level missing of a single rod can be detected even for the inner rods. At the level of 5%, the majority of the missing inner rods can not be detected at all. The most important parameters, which determine the level of statistical fluctuations, are the following:

- Activity of the fuel assembly. This can not be changed. Measurement of fuel assemblies with long cooling-times require longer measurement times.
- Count-rate of detected gamma photons. Decreasing the discrimination level would increase count-rate. Separation of the ^{154}Eu gamma rays from the ^{137}Cs gamma rays limits the use of this method. Widening the collimator slits would increase the count-rate, but degrade spatial resolution.
- Measurement (integration) time. With the detection system used in this work, the integration time was fixed to 2 seconds. Increasing this value by a factor of 4 results in decreasing the statistical noise by a factor of 2.

Table VII. *Physical parameters that influence the imaging possibility of different fuel types.*

Fuel type	Pellet diameter (mm)	Rod outer diameter (mm)	Maximum number of rods along a scanning line	$(\mu l)_{max}$
BWR 8×8	8,36	9,5	8	7,14
PWR 17×17	8,19	9,5	17	15
VVER 440	7,59	9,1	13	10,8

Table VIII. *Summary of detection probability (%) of missing inner rods for different PWR fuel types.*

Assembly type	Measurement in water[1]			Measurement in air or in water [2]
Measurement noise	1%	3%	5%	1%
17×17–25 PWR	~100%	84%	24–52% [3]	~100%
15×15–13 PWR	~100%	96%	~80%	~100%

[1] direct algorithm
[2] model based algorithm
[3] at the upper value one rod was falsely detected as missing

5.6.6 Detection probability of a missing or replaced rod for different fuel sizes

Sensitivity limit of partial defect testing for different fuel types is summarized in Table VIII. The detection threshold is set to a low value to limit the probability of false detection to 0. Main conclusions are as follows:

- For assemblies with size from 8×8 BWR to 15×15 PWR, 100% detection probability of a missing rod can be achieved if the statistical noise in the measured projections does not exceed 1%. Higher noise levels will gradually decrease detection efficincy. In any case, noise should not exceed 5%, otherwise direct image reconstruction technique can not be used. In case of 1% noise, even a visual evaluation is possible.
- The large size PWR assemblies are very sensitive to noise in the measured projections. Higher statistical noise will decrease the detection probability because missing and normal rod activities are overlapping.
- Evaluation of an image measured in air (air channel) can be made only with model-based calculations. For this algorithm the maximum allowed noise level is around 1%. Above that level the image will be very noisy.
- In case of measurements with a 1% statistical accuracy, the detection probability is very high and similar both for the measurements made in water and in air.

5.6.7 Detection probability for different configurations

The objective of a partial defect testing is to detect removal of fuel rods in fuel assemblies. Detection probability depends on the number and positions of rods removed. The main considerations are summarized in the following.

Removing rods from outer positions

Any single rod removed from the first two outer rows will be detected with 100% probability. For a 17×17 PWR assembly there are about 120 rods in these positions.

Removing a group of inner rods

Removing more than one rod from neighboring inner positions will be detected with much higher probability than a single rod. Missing of 9 rods from the central positions of a17×17 assembly can be detected with almost a 100% probability. A missing smaller group of rods, represented by Figures 23 d–e, can also be detected with a high probability.

Removing of several single rods from inner positions

Missing rods in positions separated from each other by normal rods can be detected with the same probability as detection of a missing single rod. Therefore, detection of several missing single rods is the most difficult task for partial defect verification of spent fuel.

In the case of a 17×17 PWR assembly, there are some 169 inner positions. To avoid removing of neighboring rods, about 25 single rods can be removed to make the partial defect testing more difficult. According to the measurements with a 17×17 spent fuel assembly (see paragraph 4.2) about 64% of missing inner rods, i.e. every second or third inner rod was detected using data measured under non-optimum conditions including about 4% of noise. It means that 16 of the removed 25 rods were detected and 9 remained undetected, which is about 3% of the total number of rods. By using an optimum geometry and/or by reducing the noise level, this figure can be improved significantly.

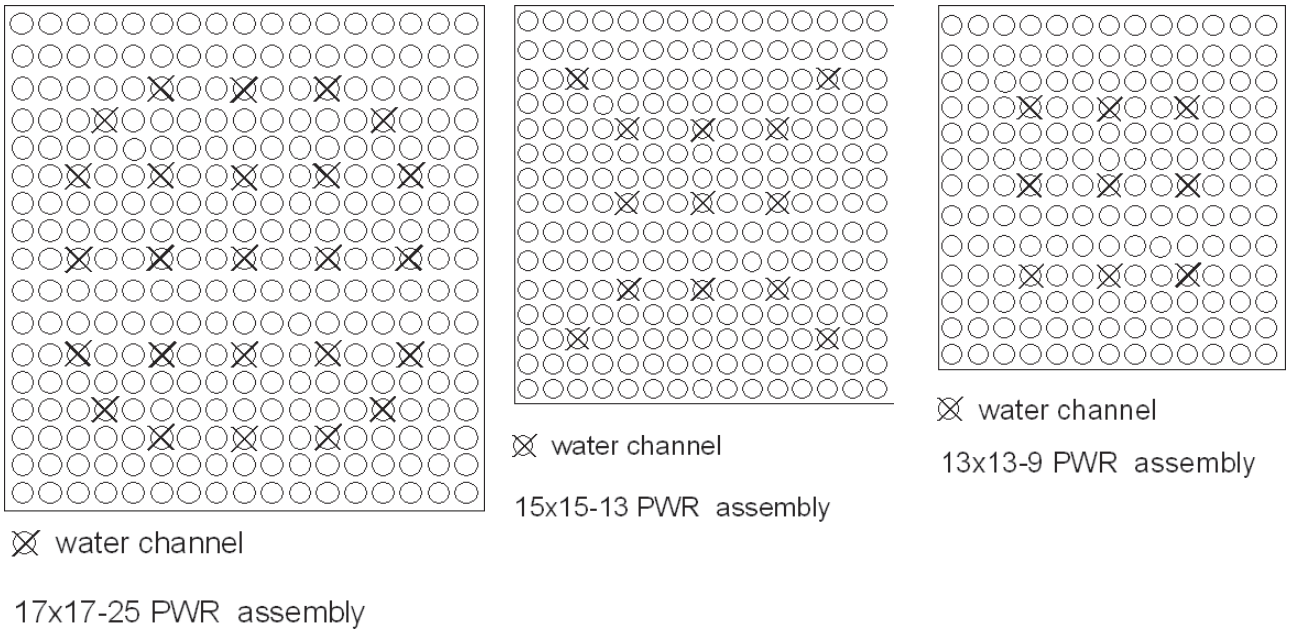

Figure 23. *Diversion scenarios to remove irradiated fuel rods from PWR and BWR assemblies..*

6 Design options for tomographic spent fuel verifier

Feasibility of the implementation of a tomographic spent fuel verifier depends not only in the detection power of the method but also realization and engineering of the device itself at nuclear facilities. Based on the experience gained in developing and implementing several spent fuel verification methods in different countries and different types of nuclear facilities, two basic engineering options have been developed and evaluated. The first method is called a fork option resembling the wide used fork detector of the IAEA. The other option is called a ring option.

6.1 Transportable underwater fork

In this option the assembly is hanging from the mast of the fuel handling machine in a fixed position during the measurement. The detector–collimator system is rotated inside the watertight, fork-shaped detector head. The measurement time is about 2 × 10 minutes using an array of about 100 detectors. Figure E1 (executive summary) shows a possible schematic design of such a tomographic verifier. Figure 24 shows the same option with a bit more in detail.

The main disadvantage of this arrangement is that one has to measure the assembly twice in order to scan over 360 degrees. In practice this means moving the assembly inside the fork for measuring the first half of the assembly. After that the assembly is moved out, rotated 180 degrees and moved in again for measurement of the second half. Exact positioning of the assembly during measurements needs to be secured mechanically. A possible advantage could be that the use of the method is similar to the use of the IAEA fork detector that is familiar to many operators.

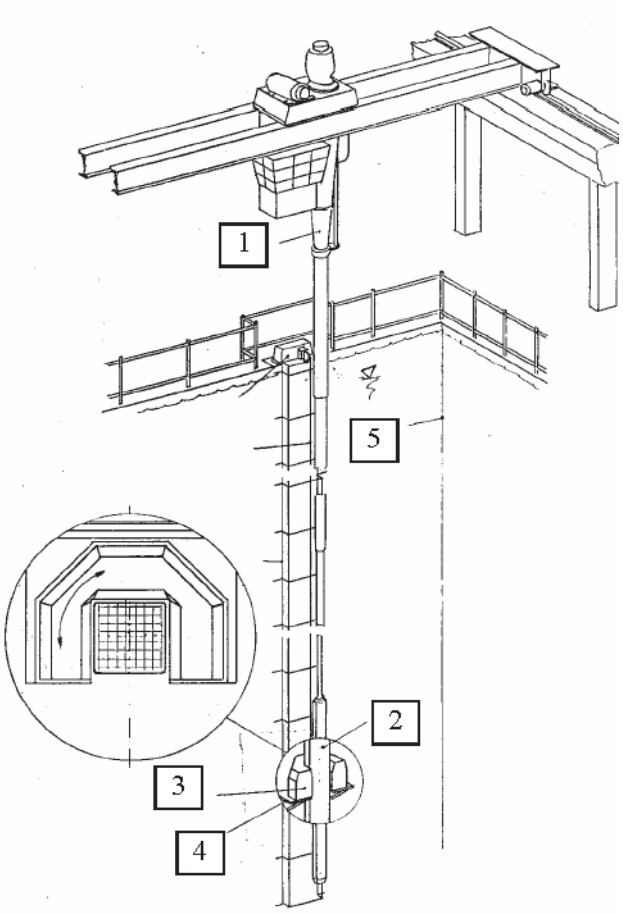

Figure 24. *Schematic fork-design of a tomographic spent fuel verifier showing the mast of the fuel handling machine (1), the fuel assembly during measurement (2), the detector head (3), the stand of the detector head (4) and the pool wall (5).*

6.2 Transportable underwater ring

In this option the assembly is in a fixed position during the measurement inside the ring-shaped detector head. The moving detector–collimator system is rotated around the whole assembly inside the detector head. The detector head can be placed into a location where the assembly can be moved inside the ring. The measurement time is about 5–15 minutes using two detector arrays each about 100 detectors. Figure E2 shows a possible design of a ring-shaped tomographic verifier. Figure 25 shows again the same option but with a bit more in detail.

In principle, the ring detector could be placed where ever the fuel assemblies can be moved inside the detector ring. One possibility could be to locate the detector above the rack in the fuel pool and lift the assembly partly inside the detector for measurement using the fuel handling machine. This approach would allow measurement of any vertical position of the assembly. Another option is to attach the detector on the pool wall and move assemblies inside the ring for measurement. During measurement the double array of detectors and collimators inside the water tight housing is rotated over 360 degrees around the measured assembly. The weight of such a detector would be about 170 kg. The measurement time for one cross section is about 5–15 minutes.

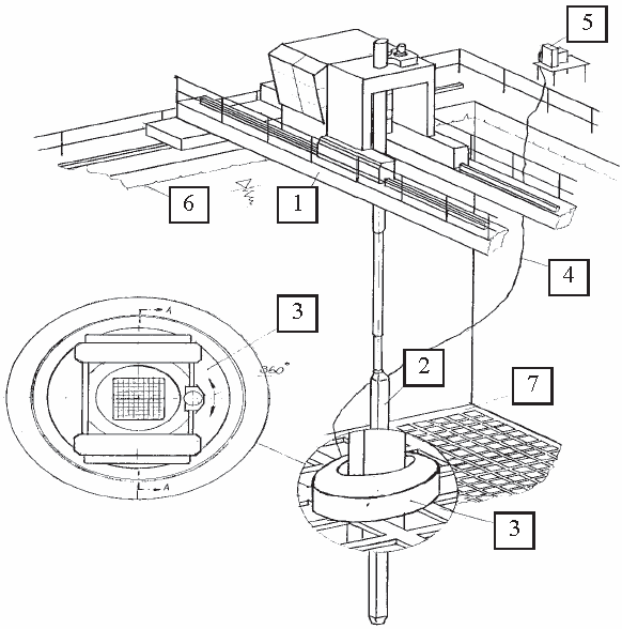

Figure 25. *Schematic ring-design of a tomographic spent fuel verifier showing the fuel handling machine (1), the fuel assembly during measurement (2), the detector head (3), a cable to the measurement electronics (4), the electronics and control of the measurement system (5), the pool wall (6) and the storage rack (7).*

7 Functional features of a tomographic verifier

7.1 Hardware

The hardware system of a tomographic verifier consists of the following components:

- A notebook PC to control the measurement and to evaluate the data.
- A docking station with commercially available computer cards. A stepper card is needed to control the stepping motors used for rotation and linear movement of the detector system.
- Motor drivers for stepping motors (commercially available).
- A gamma radiation detection unit. The unit consists of an array of room temperature semiconductor detectors with integrated electronics. The output of this unit is directly connected to the computer via a standard RS 232C or USB port.
- Stepping motors for rotation of the spent fuel assembly or the detection head and linear movement of the detectors (fork).
- A watertight underwater cable.

A block diagram for each of the two options is shown in Figures 26 and 27.

In principle, the basic features of the control units used are identical for both systems. There are, however, certain differences. The fork option has one radiation detection unit where detectors are in an array with a spacing of 4 mm. The measurement requires 2 mm sampling. With the fork option one has to move the collimator–detector system with steps of 2 mm to satisfy the sampling requirement. The fork option measurement cycle is as follows:

- measurement
- 2 mm linear movement of detector system forward
- measurement
- rotation of the detector system
- measurement
- linear movement of detector system backward
- measurement, etc.

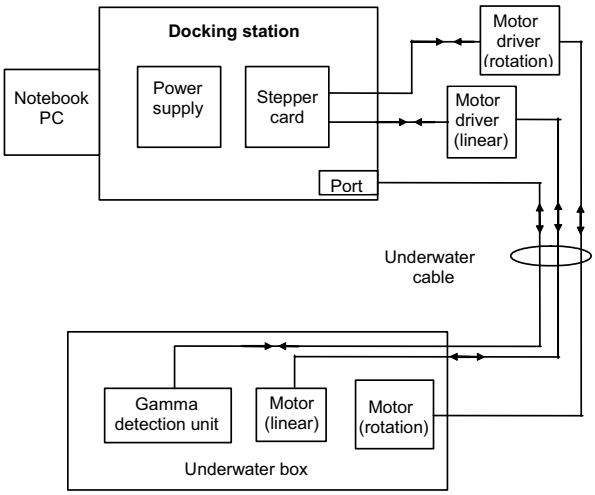

Figure 26. *A block diagram of the electric and electronic control system supporting the tomographic spent fuel verifier fork option.*

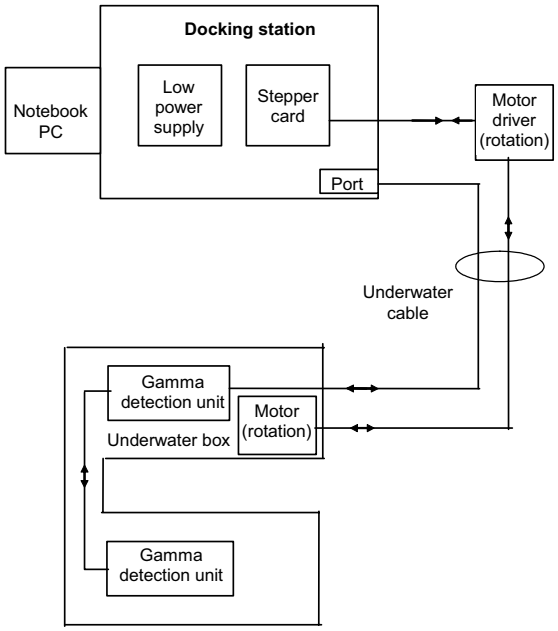

Figure 27. *A block diagram of the electric and electronic control system supporting the tomographic spent fuel verifier ring option.*

The linear movement needs an additional motor unit in the fork option. The required extra movement will increase measurement time somewhat. Both motors are inside the detector head.

In the ring option there is no need for any linear movement because the system includes two detection units on opposite sides of the measured assembly. Slits are shifted in order to measure different lines by the opposing detectors. Rotation of each array by 360 degrees will result in a scan at every 4 mm. In total, this results in the required 2 mm sampling. The motor for rotation of the detection system is inside the detection head.

7.2 Software

Two software packages are needed to use the tomographic spent fuel verifier. Fist, the control software is needed for controlling the measurement and the data collection. The measurement phase can be fully automated. Second, the image reconstruction and evaluation software is needed. The results calculation phase can also be fully automated. There are several data output options available to facilitate better interpretation and understanding of the final results obtained. Cross-sectional images as well as documented results of missing rods are available. The same notebook PC can be used for both software packages.

7.3 Operating procedures

The operating procedure for carrying out a partial defect verification of spent fuel assemblies consists of the following steps:

- check the functionality of the verifier
- install the verifier to the measurement position e.g. in the storage pool
- calibrate the equipment, if necessary (dicriminator level settings etc.)
- select the first fuel assembly and move it inside the measurement head
- make scanning measurements
- repeat measurements with other assemblies
- dismount the verifier, decontaminate and move into the storage box or location, as needed
- evaluate the measurement data and interpret the results.

The verification procedure is rather straightforward. It is the ease of operation and limited spent fuel handling that have guided the development work of the tomographic verifier concept. In general, the procedures are the same for verifying both BWR and PWR assemblies.

When using the fork option to measure PWR assemblies, the data collection must be repeated because only 270 degrees can be measured during one scanning and all sides of the assembly, 360 degrees, need to be measured.

For the ring option, only one fuel movement is needed to carry out the measurement. This may include either moving the assembly into the ring or partially raising the assembly inside the ring. All the views, over 360 degrees, can be measured during one scanning cycle. Typical measurement times, excluding the fuel handling, for the large PWR assemblies are 5–10 minutes using the the ring option and 10–20 minutes using the fork option, respectively. The measurement time depends on the required accuracy (statistical noise). Higher accuracy requires longer measurement times. In general, smaller assemblies in diameter need shorter measurement times than larger assemblies.

7.4 Additional technical options

Adding some extra components into the underwater detector head would provide new features to the tomographic verification system. These components could include**:**

- A gamma spectrometric system either using some detectors of the array or adding e.g. an extra large-size CZT detector for the gamma spectrometric use.
- Neutron detectors. The detector housing is large enough for positioning two fission chambers in a way similar to the widely used IAEA Fork detector (FDET).

These new elements would give additional data useful both for safeguards and for operational use. They include:

- Axial gamma or neutron, gross or spectral, profiles of the assembly measured.

- Excellent averaged gamma or neutron data for the whole assembly due to the fact that measurement are made in very small steps (120 views).
- Radial gamma profiles of the assembly.

In many cases spent fuel ponds are provided with operator owned equipment for fuel testing or maintenance. As an example, in Finland and in Sweden each BWR plant and AFR storage is equipped with a so-called gamma wagon to hold and rotate fuel assemblies in a special fixture. The gamma wagon is attached to the wall of the pool. These gamma wagons can be used technically to support also a tomographic verifier. Use of the existing equipment and possibilities would reduce costs of the method.

8 Cost–benefit analysis

Traditional cost–benefit analysis may not be appropriate in the safeguards use because many of the costs and benefits related to safeguards are non-quantifiable in nature. One can not give a price to a credible conclusion of the non-diversion of nuclear material. Also the costs associated with the inability to draw such a conclusion are non-quantifiable.

8.1 Methods considered

According to the safeguards criteria of the IAEA, the partial defect test for spent fuel assemblies should be able to detect if half or more of the fuel rods have been removed and possibly replaced by dummies. The possibilities to use or to develop Digital Cerenkov Viewing Device (DCVD), Fork detector (FDET), Enhanced FDET, Safeguards MOX Python (SMOPY) and High Energy Gamma Emission Tomography for partial defect test device are compared in Table IX.

The DCVD can not distinguish spent fuel rods from activated steel structures (dummies) because the detected Cerenkov light is not spent fuel specific. This is a basic limitation concerning verification of spent fuel. The fuel assembly types whose top part structure is closed can not, even in principle, be verified with the DCVD on the partial defect level. The DCVD is under further development and may in the future offer additional features for verification of fuel assemblies which are not covered. It may also be impossible to verify assemblies with partial length fuel rods with the DCVD. Because of the nature of the physical principle applied and the limited usability, the DCVD is not considered as a potential partial defect test method in the analysis below.

The IAEA needs an operator independent partial defect method. Using of operator declared data for partial defect analysis should be avoided because the diversion of fuel rods could be covered by an intelligent falsification of the operator declared data. This excludes the fork methods and the SMOPY device. Concerning the fork detector methods (FDET), there are configurations with 50% removed pins which can not be detected using the neutrons vs. gross gamma curve (4).

High Energy Gamma Emission Tomography, possibly complemented by weighing the assemblies is the only known passive method, which has potential to be developed for a reliable partial defect testing of spent LWR fuel. The tomographic method has no inherent deficiencies in verifying all possible cases of fuel items without need for operator declared data. This is why the cost–benefit analysis has been carried out including only the fork and ring design options of the tomographic device included in the report.

8.2 Comparison of tomographic fork and ring options

The following cost–benefit analysis considers the case that the operator transfers spent LWR fuel assemblies from a storage position to a difficult–to–access storage. The partial defect verification is carried out by the IAEA during the transfer operation. It is important to notice that the costs are only rough estimates. The costs and benefits of the fork and ring options are evaluated and compared with each other, when possible.

Mechanical hardware

The mechanical support structure is made of stainless steel. It has to be produced in a special way. The cost of mechanical support structure is estimated to be about 31 000 USD for both options. No quotation from manufacturer is available. It is estimated that the underwater head housing of the fork option would cost about

Table IX. *The methods considered for developing a partial defect verification method of spent LWR fuel for the IAEA.*

Method	Burnup limitations	Cooling time limitations	Which part of assembly can be verified	Operator declared data needed	Potential for real partial defect method for spent fuel
DCVD	no	no	upper end	no	limited
FDET	> 18 MWd/kgU	> 10 a	any	yes	no
Enhanced FDET	> 18 MWd/kgU	no	any	yes	no
SMOPY	no	< 7–9 a	any	yes	no
Gamma emission tomography	no	no	any	no	yes

6 000 USD. The underwater head housing of the ring option would cost about 4 500 USD. The cost of the transport case of the device is estimated be about 1 500 USD.

Detectors, collimators and electronics
A detection unit contains CdZnTe (CZT) detectors, collimators and electronics. One detection unit is needed for the fork option and two detection units for the ring option. According to the cost estimates done by the Baltic Scientific Instruments (BSI), the detection unit with 104 channels would cost about 137 200 USD. The cost of two units with 104 channels would be about 221 300 USD.

Cables and connectors
The cost of cables and connectors is estimated to be about 2 500 USD. No quotation from a manufacturer is available.

Motors and drivers
One motor and one driver are needed for rotation the detection system. They are identical for the fork and the ring option. The stepping motor would cost about 380 USD and the driver would cost about 710 USD. An additional motor and driver are needed for the linear movement of the detection unit in the fork option. The motor would cost about 260 USD and the driver would cost about 580 USD.

Computer hardware
The computer expenses are estimated to be about 2 500 USD. The costs of the computer cards would be about 1 000 USD. One computer is needed for measurement control and for evaluation of the data for both design options.

Computer software
The price of the computer software is approximately the same for both design options. The price of the control software is estimated to be about 10 000 USD. The price of the image calculation and evaluation software can be estimated to be about 25 000 USD.

Operation and maintenance
The authorization requirements of the IAEA aim to ensure the quality of newly acquired equipment. The acceptance and field testing of the device are normally done within the framework of the MSSP support programme task of the IAEA under which the device has been developed. Other tests like operational, thermal, humidity and mechanical tests could be performed under the corresponding support programme. In this case there would be no direct expenses to the IAEA. If the IAEA had to do the tests alone, the costs would be about 20 000 – 30 000 USD. This unfavourable case has been used in the analysis. Due to the rough estimate the differences in the testing expenses between the fork and ring options can be neglected. It is assumed that there would be no expenses to the IAEA concerning the licensing and acceptance made by the plant operators.

One training course in the data analysis is assumed to be needed and arranged under a support programme task. One course is estimated to take about three days. Five inspectors could participate in the course. The traveling cost is estimated to be about 1 000 USD per inspector. The cost of one training day per inspector is estimated to be 1 500 USD. The expenses of a three days' training course for five inspectors would be about 27 500 USD.

The duration of an inspection campaign depends on the amount of transferred assemblies the inspector has to verify. One inspector is assumed to perform the verification measurements. Depending on the country, the cost of one inspection day is about 1 500 – 2 000 USD. To take into account the increase in costs, 2 000 USD has been used as the cost of one inspection day. Travel expenses of the inspector are estimated to be about 1 000 USD per inspection. The transport costs of the device are estimated to be about 1 000 USD per inspection.

Other features

Only the features, which are different for fork and ring options have been taken into consideration in the benefit analysis.

Placing an assembly into the measurement position has no differences between the fork and ring options from the safety point of view. The operation can be considered as normal facility operation for both options.

Installation and disassembling times are approximately the same for the fork and for the ring option. It is assumed that one day during the inspection campaign is needed for the installation, disassembling and different kind of preparation work. The measurement time with the ring option is about 10 minutes per assembly. The measurement time with the fork is about 25 minutes i.e. 2.5 times as long as it is with the ring option. It is assumed that the transfer operations take about 20 minutes per assembly. The different measurement times have been taken into consideration in the inspection campaign costs.

The aim of the operator is to transfer the spent fuel assemblies into a difficult–to–access storage effectively and efficiently. This is why it is preferable also for the operator that the measurement time is as short as possible. This benefit is estimated to be for the ring option 2 times as good as it is for the fork option.

The weight of the ring option is about 1.2 times the weight of the fork option when all components of the measurement system are taken into consideration. The transportability of the fork has been estimated to be 1.2 times better than it is for the ring option.

Summary

In all, the estimated price would be about 218 600 USD for the fork device and about 300 400 USD for the ring device. If the licensing costs of the prototype and the training costs, i.e. about 57 500 USD, would be included in the estimates the total cost would be about 276 100 USD for the fork and 357 900 USD for the ring. According to the analysis the fork device would be about 82 000 USD more economical than the ring device (see Table X). The cost of the detection unit is the dominating factor in the total costs of the both options (see Table XI). All costs have been divided over three years in the analysis.

The inspection campaigns are more economical to perform with the ring option than with the fork option (see Table XII). If, for example, 64 assemblies had to be verified, about a 5 days inspection campaign would be needed with the ring and about a 7 days inspection campaign with the fork. The measurement campaign performed with the ring would be about 4 000 USD more economical if compared to the measurement campaign performed with the fork. After about 21 measurement campaigns the inspection costs would be approximately 84 000 USD less for the ring than for the fork. If these kinds of campaigns were performed seven per year, the ring option would become a more economical option compared to the fork after about three years.

The summary of the cost–benefit analysis is shown in Table XIII. It is a rough cost–benefit approximation about three years after the IAEA would have bought the verification device.

Table X. *The cost estimates of different components of the fork and ring options in USD.*

No.	Component	Costs (USD) Fork	Ring
1	Detector, electronics and collimator system	137 200	221 300
2	Mechanical support structure	31 000	31 000
3	Underwater detector head housing	6 000	4 500
4	Motors	640	380
5	Drivers	1290	710
6	Cables and connectors	2 500	2 500
7	Computer	2 500	2 500
8	Computer cards	1 000	1 000
9	Software	35 000	35 000
10	Transport case	1 500	1 500
11	Total costs	218 630	300 390

Table XI. *The relative costs of different components of the fork and ring options in %.*

No.	Component	Relative costs (%) Fork	Ring
1	Detector, electronics and collimator system	62,8	73,7
2	Mechanical support structure	14.2	10,3
3	Underwater detector head housing	2,7	1,5
4	Motors	0,3	0,2
5	Drivers	0,6	0,2
6	Cables and connectors	1,1	0,8
7	Computer	1,1	0,8
8	Computer cards	0,5	0,3
9	Software	16,0	11,7
10	Transport case	0,7	0,5
11	Total	100	100

Table XII. *The cost estimates in USD for an inspection campaign using the fork and the ring option.*

No.	Component	Relative costs (%) Fork	Ring
1	Costs of one inspection day	2 000	2 000
2	Number of days per inspection	7	5
3	Travel costs per inspection per inspector	1 000	1 000
4	Transport costs of verifier per inspection	1 000	1 000
5	Costs of one inspection campaign	16 000	12 000
6	Number of inspections	21	21
7	Total costs of 21 inspections	336 000	252 000

Table XIII. *Summary of costs and benefits after three years of inspection use by the IAEA. Mainly the higher usability (less intrusion) results in recommending the ring option.*

No.	Parameter	Weighting	Score Fork	Ring	Weighted score Fork	Ring
1	Transportability	10%	1,2	1	0,12	0,10
2	Intrusiveness	10%	2	4	0,20	0,40
3	Costs	80%	1,0	1,1	0,80	0,81
Total		100%			**1,12**	**1,31**

9 Conclusions and recommendations

It can be concluded from the simulation and experimental studies on several BWR and PWR assemblies that the method based on the gamma emission tomography is feasible and capable for making partial defect testing of spent LWR assemblies. Under optimized conditions, which are technically achievable, even the large 17×17 PWR assemblies can be verified at a single rod level. This requires, among other things, limiting the statistical noise of the measurements down to the 1% level.

If missing or replacement of a single rod is not required to detect, the proposed tomographic method can be used also at a higher statistical noise level (up to 5%). This would result in a detection sensitivity that is worse than the single rod level but still an order of magnitude better than required by the present 50% criteria for partial defects of spent fuel. At the moment, the IAEA has no verification methods that are capable for verification that 50% or more of the irradiated fuel rods have been replaced or missing from spent LWR fuel assemblies.

Due to the fact that simulation results could be confirmed by experimental results, it is considered sound to propose designing and construction of a prototype tomographic verifier and to select a test facility, where the prototype and the verification procedures could be tested in realistic conditions. For further development, the ring option is recommended as the principle of the prototype tomographic verifier.

According to the agreed Task Outline, the Agency is expected to evaluate the results included in the report and to make a decision on the continuation of the task. The next phase would thus be to design and construct a prototype of the proposed tomographic verifier.

Acknowledgements

The authors would like to thank Mr. Asko Turunen, STUK, for taking part in the development work by designing the conceptual engineering drawings of possible inspection use tomographic verifiers. The authors are grateful also to the overall support provided during the field exercises by the operators of the TVO KPA-store, Finland and Ringhals NPP in Sweden.

References

1. Lévai F, Dési S, Tarvainen M, Arlt R, Use of high energy gamma emission tomography for partial defect verification of spent fuel assemblies. Final report on the Task FIN A98 of the Finnish Support Programme to the IAEA Safeguards, Report STUK-YTO-TR 56, Radiation and Nuclear Safety Authority, Helsinki 1993.

2. Tarvainen M, Lévai F, Valentine T, Abhold M, Moran B, NDA techniques for spent fuel verification and monitoring, Report on Activities 6a and 6b of Task JNT C799 (SAGOR), Finnish Support Programme to the IAEA Safeguards, STUK-YTO-TR 133, Helsinki 1997.

3. Lévai F, Honkamaa T, Tarvainen M, Larsson M, Rialhe A, Jacobsson S. An Exercise for Partial Defect testing of a PWR Assembly by Underwater Tomography. Proceedings of Symposium on International Safeguards, Verification and Nuclear Material Security, IAEA-SM-367/CD 01-04527, Paper 14/6 (8 pp), IAEA Vienna 29.10.–2.11.2001.

4. Tiitta A, Saarinen J, Tarvainen M, Jansson K, Jansson P, Carchon R, Gerits J, Koulikov I, Lee YG. Investigation on the possibility to use fork detector for partial defect verification of spent LWR fuel assemblies, Final report on Task JNT A 1071, STUK-YTO-TR 191, Helsinki 2002.

5. Staffan Jacobsson, Ane Håkansson, Camilla Andersson, Peter Jansson, Anders Bäcklin. A Tomographic Method for Verification of the Integrity of Spent Nuclear Fuel. SKI Research Report 98:17, 1998.

STUK-YTO-TR 189—ANNEX

SAFEGUARD ANALYSIS OF TOMOGRAPHIC DATA FROM A MEASUREMENT ON A PWR NUCLEAR FUEL ASSEMBLY

Staffan Jacobsson

Uppsala University

Contents

1 Introduction

In March 2001, tomographic measurements were performed at the Ringhals 4 nuclear power plant in Sweden. The measurements were carried out on a PWR fuel assembly using portable equipment, which is described in ref. /1/. Analysis of the data is also described in ref. /1/.

The additional analysis described in this report has been performed with an alternative tomographic method. It was originally developed in an investigation of the applicability of tomography for verification of the integrity of nuclear fuel, performed by Uppsala University for the Swedish Nuclear Power Inspectorate (SKI), ref. /2/.

The method has since then been further developed for tomographic measurements of the relative pin power with high accuracy (1–2 %, 1 S.D.). For this purpose, a high-precision device has been constructed, described in ref. /3/. Having a weight of 27 tonnes, the device is not intended for inspection purposes although it is still transportable.

Some differences are discussed below between the conditions for a portable device, with which the data analysed in this report has been collected, and the type of device for which the algorithm has been developed. Also implications on the analysis are accounted for.

2 Tomographic method

2.1 General remarks

As mentioned above, the algorithm is developed for a heavy, high-precision device. The method involves detailed modelling of the gamma-ray interaction of the emitted radiation from the fuel. The most prominent properties of the analysis method are:

- A point-kernel method is utilised, i.e. only full-energy transport of gamma rays is modelled.
- The geometry of both the measured assembly and the measurement equipment are utilised.

The first item originates in that the method is designed for a measurement system involving spectroscopic analysis of the full-energy peak of the selected decay. This is further discussed in section 5.2.

The second item implies that geometric information of high accuracy is desired for the equipment and its position for each data point. It also involves utilisation of the nominal geometry of the assembly, i.e. the fuel matrix is assumed to be complete.

The result of such an assumption for an assembly where removed and/or replaced rods occur has been extensively investigated in ref. /2/. Results have been presented from simulations as well as laboratory measurements and measurements on a spent fuel assembly. (Refs. /2/, /4/, /5/ and /6/.) Concluding these investigations, both the 662 keV gamma-ray energy from ^{137}Cs and the 1274 keV energy from ^{154}Eu should be applicable for BWR fuel. However, the results indicate that gamma rays of the higher energy may have to be used for confident detection of removed rods in PWR fuel.

2.2 Tomographic algorithm

The algorithm is of the algebraic type. The fraction w_{mn} of gamma quanta emitted from a certain picture element n that reaches the detector in a certain position m is calculated theoretically. This is done by modelling the measuring geometry and full-energy transport for gamma rays of a selected decay from the fuel to the detector. An equation system is obtained:

$$\begin{pmatrix} w_{11} & w_{12} & w_{13} & \cdots & w_{1N} \\ w_{21} & w_{22} & w_{23} & \cdots & w_{2N} \\ w_{31} & w_{32} & w_{33} & \cdots & w_{3N} \\ \cdot & & & & \\ w_{M1} & w_{M2} & w_{M3} & & w_{MN} \end{pmatrix} \begin{pmatrix} A_1 \\ A_2 \\ A_3 \\ \cdot \\ A_M \end{pmatrix} = \begin{pmatrix} I_1 \\ I_2 \\ I_3 \\ \cdot \\ I_M \end{pmatrix}$$

where w_{mn} = contribution coefficient of measuring position m from pixel n.
A_n = activity in pixel n.
I_m = intensity of measuring position m.

The equation system should be overdetermined, i.e. the number of measuring positions M should be larger than the number of pixels N.

Generally, transmission through the collimator is neglected and contributions from gamma-ray scattering into the detector are excluded. However, transmission may be evident in a relatively light collimator and scattering will affect the measurements if no spectroscopic peak analysis is performed. It can be noted that both these circumstances occur in the measurements analysed in this report. Such contributions may to some extent also be included in the model, but that has so far not been made.

3 Analysed measurement data

Measurements of the radiation field from a PWR fuel assembly were performed in March 2001 at the Ringhals 4 nuclear power plant in Sweden. The measurements are described in ref. /1/ together with tomographic analysis of the data. The data was later submitted to Uppsala University, Sweden, for an alternative analysis accounted for in this report.

3.1 Measured fuel assembly

A spent 17×17 PWR assembly of the AFA-S type, manufactured by Framatome, was measured. The nominal cross section is illustrated in Figure A1. A system of coordinates for defining the position of each rod is introduced in the figure.

The measured assembly had a cooling time of about 7 years. It had five peripheral rods exchanged, positions T2, T4 and T15 with depleted uranium rods and positions T9 and T10 with dummy rods of homogeneous stainless steel.

As illustrated in Figure A1, this type of assembly has 25 water channels in its interior, i.e. water-filled zircaloy tubes with slightly larger diameter than the fuel rods. 24 of these are guide tubes for control rods and one (position K9) is an instrumentation tube. For simplicity, all these will be referred to as water channels.

3.2 Data set analysed

The measurement equipment and its geometry is described in ref. /1/. The measurements were performed at an axial position near the lower end of the assembly. The gamma-radiation field was recorded in 120 angles relative to the assembly. This was achieved by rotating the assembly with an angular step of 3°. For each angular position 155 lateral positions were recorded with a lateral step of 2 mm, achieved by translating the detector package. Thus the radiation field was recorded in 18 600 positions relative to the assembly.

As described in ref. /1/, CZT detectors were used in the measurements. These detectors have very low peak efficiency, implying that the primary data mainly consisted of Compton events in the detectors. As discussed in section 2, this is not in accordance with the conditions for which the analysis code used in this work was developed. A more elaborate discussion on the consequences of this can be found in section 5.2.

To select Compton events in the detector from the interaction of 1274 keV gamma quanta (emitted in the decay of 154Eu), a lower discriminator level was applied at about 400 keV and a higher level at about 700 keV. However, the data set used for this analysis was the set from the upper discriminator, as it was considered most appropri-

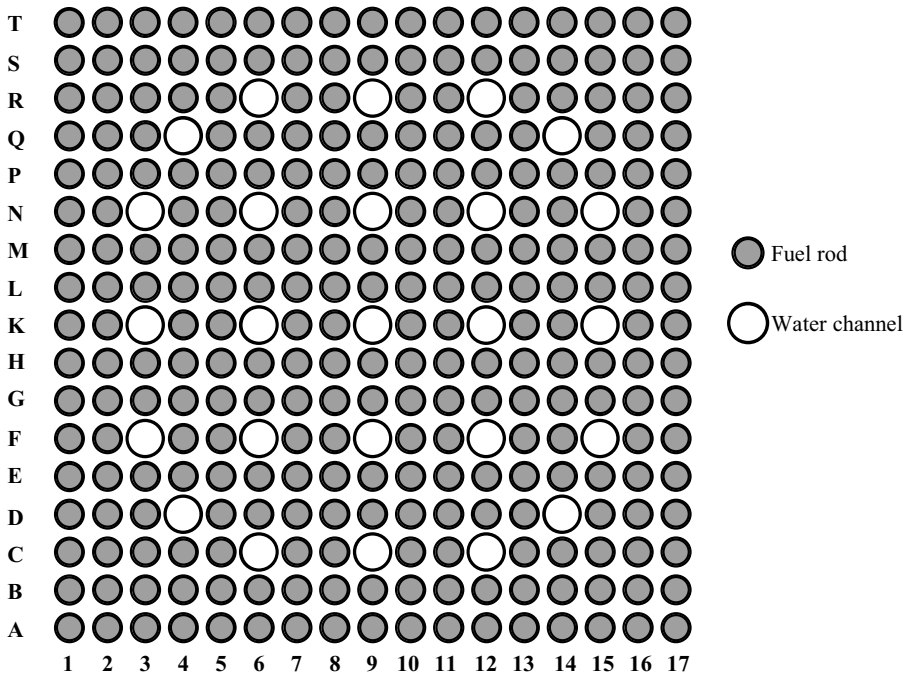

Figure A1. *The cross section of the PWR 17×17 fuel assembly. Note the system of coordinates introduced for defining the position of each rod.*

Table A-I. *Positioning data extracted from the measurements.*

Assembly centre (x) [mm]	Assembly centre (y) [mm]	Angular offset [°]	Translation offset [mm]
0.81 ± 0.26	2.08 ± 0.36	–0.37 ± 0.12	–0.76 ± 0.10

ate for this analysis method.

Further on, the data analysed in this report had been subject to subtraction from the estimated contribution of scattered events. The author of this report has no information of how the subtraction procedure had been performed.

4 Analysis

To perform tomographic analysis with the method described in section 2, detailed geometric information is required. Thus the position of the fuel assembly relative to the measurement equipment had to be extracted before applying the tomographic reconstruction algorithm. The positioning analysis is accounted for in section 4.1 while the results of the tomographic analysis are accounted for in section 4.2.

4.1 Positioning

Required positioning data for the assembly could be extracted from the measured data set. This was done by analysing variations of the intensity distribution in rotations about each of the four angles where one side of the fuel assembly is perpendicular to the symmetry axis of the collimator. In such an angle, the projected width of the lateral intensity distribution has a minimum. The following quantities could be determined:

- The angular offset of the assembly rotation.
- The lateral position of the assembly centre relative to the rotation centre in two dimensions.
- The translation offset. It is here defined as the distance between the detector transversal "zero" position relative to the assembly rotation centre and is a property of the equipment.

The extracted positioning data are accounted for in Table A-I.

The uncertainties stated in Table A-1 reflect variations obtained when performing multiple analysis of the data set, varying the intensity level defining the projected width. Possible systematic errors are not included.

The stated accuracy of the rotation equipment was 0.5° and the stated accuracy of the lateral positioning of the detectors was 0.05 mm. With exception of the latter figure, the reconstruction procedure would benefit from better positioning accuracy.

4.2 Tomographic results

4.2.1 General remarks

The investigations were primarily concentrated on the ability to detect the five exchanged rods in the assembly, see section 3.1. This investigation is accounted for in section 4.2.2.

However, also the ability to detect the 25 water channels was considered of interest, as they can represent removal of rods from the assembly interior. According to section 2, the nominal geometry of the assembly is utilised in the tomographic algorithm, meaning that the presence of these water channels is known and thus, by default, no activity will be assigned to these positions. To perform such an investigation, an artificial type of fuel was implemented in the software having rods in all positions, i.e. even in the positions of the 25 water channels. The ability to detect the water channels under those circumstances was studied. This investigation is accounted for in section 4.2.3.

According to the discussion in ref. /2/, the reconstruction algorithm is expected to return an activity close to zero in the position of a non-active normal rod. A slightly larger value is expected in the position of a rod exchanged with a lighter material (such as a dummy rod of homogeneous stainless steel). Further on, the depleted uranium rods present in this fuel assembly can be expected to contain substantially lower activities than a normal rod, which should also be readily detected.

If a rod has been removed, i.e. not replaced, a situation similar to having a water channel in such a position occurs. In such a case, a finite reconstructed activity is expected. According to ref. /2/ also such removal should be readily detected, provided that a relatively high gamma-ray energy is utilised.

4.2.2 Detection of the exchanged rods

First an analysis was performed where the nominal geometry of the fuel was modelled. The reconstructed activity distribution can be found in Figure A2. The picture has been shaded according to the reconstructed source concentration in each rod. White represents zero activity and black represents maximum activity.

As can be seen in Figure A2, the exchanged rods in positions T2, T4, T9, T10 and T15 are clearly visible. However, the relevant parameter in this study is the confidence level for which a missing or replaced fuel rod can be detected. This parameter may be measured in the number of standard deviations (S. D.) of a specific fuel rod from the average rod activity. To illustrate this, Figure A3 shows the distribution of the reconstructed activities in different positions. The average activity in all positions has been set to 1.0.

According to Figure A3, the reconstructed activities in the normal fuel rods are distributed approximately according to a normal distribution. The relative standard deviation is 13 %. It should be noted that the power load in PWR fuel is generally relatively uniform, typically with a maximum power load within 10 % from average. The spread is thus larger than what is expected, indicating that the precision in the reconstructed activities of the normal rods is relatively poor. A more narrow distribution of the normal rods can be expected if properties such as high positioning accuracy, detectors with high peak efficiency and spectroscopic data collection can be realised. A more elaborate discussion on this subject can be found in section 5.

Anyway, the activities in the exchanged rods range from 6.4 S.D. to 7.4 S.D. lower than the average of the normal rods, which implies highly confident detection. However, it can be noted that one normal rod, in position N8 next to a water channel, obtains an activity 4.0 S.D. smaller than average, which could imply erroneous detection as a missing rod. The poor geometric accuracy could be a reason for this.

4.2.3 Detection of the water channels

The second step was to investigate the possibility to detect the 25 water channels, representing detection of removed rods. For this investigation, a fuel geometry with normal fuel rods in all positions was assumed in the reconstruction procedure. A histogram of the reconstructed activities in different rods is accounted for in Figure A4.

The relative standard deviation of the reconstructed activities in the normal rods is now 14 %. The reconstructed activities in the water channels exhibit a similar distribution, however with an average 2.2 S.D. smaller than the average of the

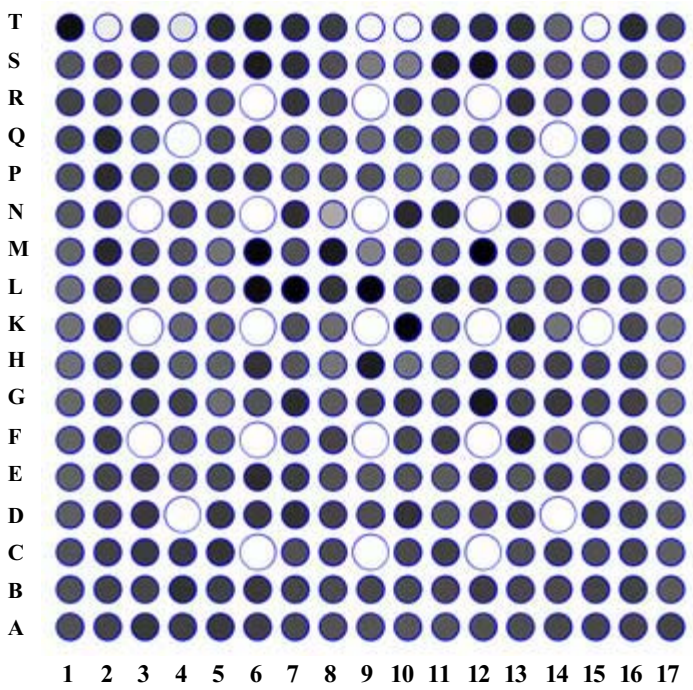

Figure A2. *Reconstructed activity distribution obtained assuming nominal fuel geometry.*

normal fuel rods. According to the normal distribution, the probability for such a deviation is 1.4 %, corresponding to four rods in a normal fuel assembly. In accordance with this, four normal rods are reconstructed to smaller values than the average of the water channels.

Anyway, Figure A4 shows that the water channels cannot be distinguished from the normal fuel rods with the current measurement precision. Provided that the accuracy can be improved, the obtained average value of the water channels indicates that these should thus be readily detected.

It should be noted that the activities in the exchanged positions range between 6.0 and 7.0 S.D. smaller than average, again implying highly confident detection.

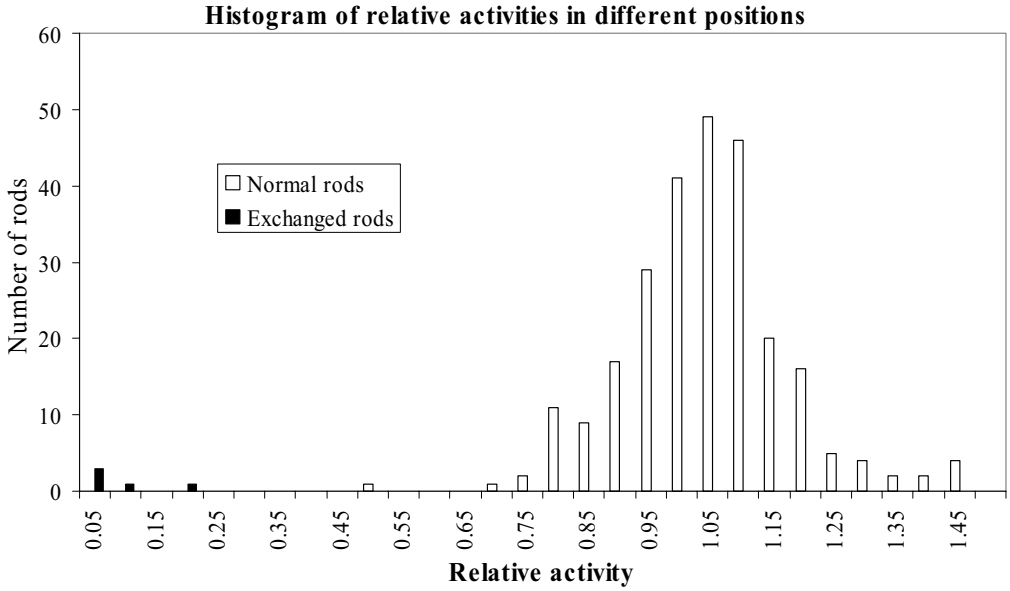

Figure A3. *A histogram of reconstructed activities in different positions, assuming nominal fuel geometry.*

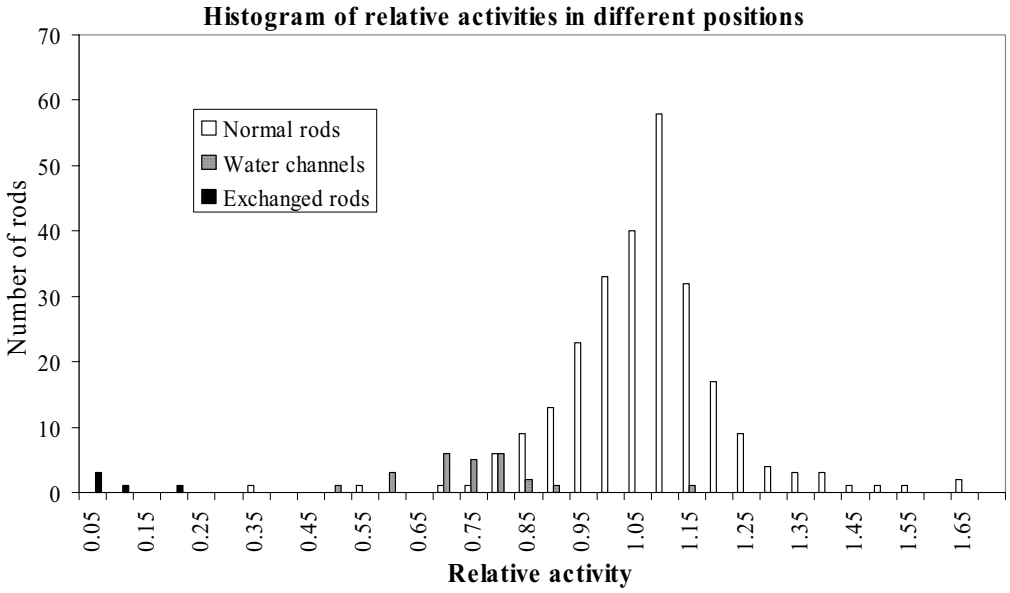

Figure A4. *Histogram of reconstructed activities in different positions assuming a fuel geometry with fuel rods in all positions.*

5 Possible ways to improve the precision

5.1 Mechanical features

A portable device has to be reasonably lightweight in order to make transportation between different sites practicable. Naturally, this implies that the dimensions and weight of various components have to be minimised. For instance, one has to minimise the shielding of the detectors, which may lead to relatively high levels of background radiation. Further on, portable equipment has to be designed to allow for installing and re-installing of the device, which affects the achievable geometric accuracy.

Still, these two items, minimisation of background in order to improve the signal-to-noise ratio and improving of the geometric accuracy, may be crucial to improve the precision.

5.2 Detectors and data collection

It is desirable to select gamma rays of certain energy in the detector/data collection system. The two main reasons for this are:

I. The interaction of gamma rays with matter has to be taken into account accurately in the tomographic procedure in order to obtain accurate results. Since this interaction is energy dependent, spectroscopic measurements are clearly advantageous.

II. Different isotopes have different distributions within the assembly due to differences in burn-up, enrichment, etc. To avoid multiple components in the measured data, spectroscopic measurements should be used to select specific decays from various isotopes.

To illustrate the discussion, an example of a gamma-ray spectrum from a BWR assembly with 8 years cooling time, collected with a high-resolution HPGe detector, is presented in Figure A5. Two peaks relevant for safeguard measurements are indicated in the figure, namely the 137Cs peak at 662 keV and the 154Eu peak at 1274 keV. As is obvious from Figure A5, the large number of peaks from different decays makes high resolution desirable in order to select the decay of interest.

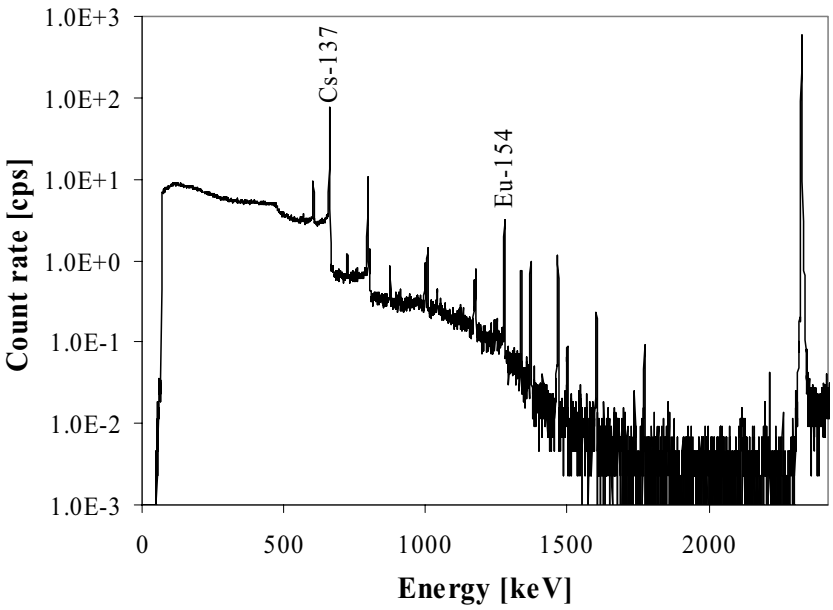

Figure A5. *A spectrum from a BWR assembly with a cooling time of 8 years, measured with an HPGe detector. Two peaks relevant for safeguard measurements, the 662 keV peak from ^{137}Cs and the 1274 keV peak from ^{154}Eu, are indicated in the figure. The peak to the right is an artificial pulser peak.*

An optimum would be to use detectors with high resolution and high peak efficiency together with spectroscopic analysis. The main features of such a system are:

- High resolution leads to small width of each peak and thus the decay of interest can be selected with high specificity.
- High peak efficiency leads to large peaks and small background, i.e. high signal-to-noise ratio.

Although both high resolution and high peak efficiency may be difficult to achieve in practice, one should be aware of that better precision could be obtained by using a detection system with such properties. The spectrum in Figure A5 clearly shows that analysis based on events in the Compton background will lead to multiple components in the data.

6 Discussion on evaluation of data

It may be argued that an inspector would require some automatic evaluation of the results from this type of analysis. In the evaluation this type of data, two situations can be foreseen:

- Operator-declared data of the fuel are available.
- No operator-declared data are available.

If operator-declared data are available, measurements can be used to verify these. The most important measurement property would then be the precision in reconstructed relative activities for normal rods. Even relatively small deviations from operator-declared data would then be significant and confident detection of removed or replaced rods would be expected.

However, if no operator-declared data are available, the evaluation will have to be based on deviations from average reconstructed activity and on subjective apprehension of the reconstructed picture. There is a risk that such a procedure may lead to erroneous statements. Some PWR assemblies e.g. contain rods of depleted uranium with a content of burnable absorbers, so called BA rods. These are used for keeping the reactivity at a desired level in the beginning of the fuel cycle and generally obtain substantially lower activities than normal rods during operation. These would likely be detected as removed or replaced, although their presence is in accordance with normal operation.

It may thus argued from a measurement point-of-view that it is desirable to base tomographic safeguard measurements on verification of operator-declared data.

7 Conclusions

The presented tomographic analysis method has been applied on measurement data collected at the Ringhals 4 nuclear power plant. The analyses have clearly revealed five exchanged rods in the measured fuel assembly. The average reconstructed activities of these have been between 6.0 and 7.4 S.D. lower than the average of the normal rods.

Also the water channels have been indicated, with an average reconstructed activity 2.2 S.D. lower than the normal fuel rods. However, the precision has to be improved to allow for confident detection.

It has been argued that a higher detection level can be expected using a device where properties such as high positioning accuracy, detectors with high peak efficiency and spectroscopic data collection are easier to realise. The results indicate that even the removal of a single, central rod may be confidently detected provided that the precision can be improved.

It has also been pointed out that the presence of rods with significantly lower activities than normal rods, e.g. BA rods of depleted uranium, may be in accordance with normal operation. It has therefore been argued from a measurement point-of-view that it is desirable to base tomographic safeguard measurements on verification of operator-declared data.

8 References

/1/ F. Lévai, T. Honkamaa, M. Tarvainen, M. Larsson, A. Rialhe, "An exercise for partial defect testing of a 17×17 PWR assembly by underwater tomography", IAEA Symposium in International Safeguards, Vienna, October 2001.

/2/ S. Jacobsson, A. Håkansson, C. Andersson, P. Jansson, A. Bäcklin. "A Tomographic Method for Verification of the Integrity of Nuclear Fuel", SKI Report 98:17, ISSN 1104-1374, March 1998.

/3/ P. Jansson, S. Jacobsson, A. Håkansson, A. Bäcklin. "PLUTO—A Device for Tomographic Determination of the Power Distribution in Nuclear Fuel Assemblies". To be published.

/4/ S. Jacobsson, A. Håkansson, C. Andersson, P. Jansson, A. Bäcklin. "A Tomographic Method for Experimental Verification of the Integrity of Spent Nuclear Fuel", Applied Radiation and Isotopes Vol. 53, No 4–5, October-November 2000, New York, ISSN 0969-8043, pp. 681–689.

/5/ S. Jacobsson, C. Andersson, A. Håkansson, A. Bäcklin. "A Tomographic Method for Verification of the Integrity of Spent Nuclear Fuel Assemblies – I: Simulation Studies", Nuclear Technology, vol. 135, no 2, August 2001, pp. 131–145. ISSN: 0029–5450.

/6/ S. Jacobsson, A. Håkansson, P. Jansson, A. Bäcklin. "A Tomographic Method for Verification of the Integrity of Spent Nuclear Fuel Assemblies - II: Experimental Investigation", Nuclear Technology, vol. 135, no 2, August 2001, p. 146–153. ISSN: 0029–5450.